Supporting Information

Proton Reduction by Bimetallic Zinc Selenolate Electrocatalyst

Aditya Upadhyay,[a] *Saurav K. V.,*[a] *Evelin Lilly Varghese,*[a] *Ananda S. Hodage,*[a] *Amit Paul,*[a] *Mahendra Kumar Awasthi,*[b] *Sanjay Kumar Singh,*[b] *and Sangit Kumar*[*]

[a] Department of Chemistry, Indian Institute of Science Education and Research, Bhopal By-Pass Road, Bhauri, Bhopal 462 066, Madhya Pradesh, India

[b] Department of Chemistry, Indian Institute of Technology Indore, Khandwa Road, Simrol, Indore 453552, Madhya Pradesh, India

Table of Contents

Supplementary Test

Methods

Representative Procedure. To the stirred solution of schiff base diselenide **2** (248 mg, 0.45 mmol, 1 equiv.) in ethanol, we added sodium borohydride (76 mg, 2.0 mmol, 4 equiv) to generated in-situ selenol and stirred the solution up to 4 h at room temperature. Then we added zinc chloride (122 mg, 0.9 mmol, 2 equiv) and stirred the solution for 2 h. After that, the solvent was removed by the rotatory evaporator, and the solid residue was washed with aqueous sodium bicarbonate solution several times to afford a light yellow colored novel bimetallic zinc selenolate complex **1** in (230 mg) 75% yield. Crystallization was done in DMSO water (2:1) mixture to afford yellow-colored crystals.

Electrochemistry. A potentiostat (CHI700E Biopotentiostat Instrument was used for electrochemical measurements. The three-electrode electrochemical cell consisted of a Glassy carbon (3 mm Diameter, 0.07 cm^2) as the working electrode, a nonaqueous $Ag/AgNO_3$ (10 mM $AgNO_3$) and aqueous Ag/AgCl (0.1 M KCl) as a reference electrode, and a platinum wire as a counter electrode were used for the electrochemical measurements. All experiments were repeated at least twice to check their reproducibility.

Determination of transfer coefficient (α): Using Laviron's method,[2] from the cathodic and anodic peak potentials, the transfer coefficient (α) can be determined using the eq (1) and (2):

$$E_{pc} = E - \left(\frac{RT}{\alpha nF}\right) \ln\left[\frac{\alpha nF}{RTk_{app}}\right] - \left(\frac{RT}{\alpha nF}\right) \ln \nu \qquad (1)$$

$$E_{pa} = E - \left(\frac{RT}{\alpha nF}\right) \ln\left[\frac{\alpha nF}{RTk_{app}}\right] - \left(\frac{RT}{(1-\alpha)nF}\right) \ln \nu \qquad (2)$$

The plot of E_{pc} and E_{pa} with respect to ln(ν) is linear. The ratio of the slopes of the cathodic and anodic peak potentials yields the value of α (Figure S6C and S7C). The result shows that the catalyst **1** and ligand **3** has α value of 0.4 and 0.3.

Determination of diffusion constant (D_0) for zinc selenolate catalyst 1:

From the Randles-Ševčík equation, eq (3), for n_p electron diffusional process, it was possible to obtain an apparent diffusion coefficient, Do.[1]

$$i_p = 2.69 \times 10^5 A {n_p}^{1.5} [cat] \sqrt{D_0 \nu \alpha} \qquad (3)$$

Here, i_p = peak current (μA), .n_p = total number of electrons transferred, A = electrode area in cm^2, [cat] =bulk concentration of the analyte (mol/cm^3), α = transfer coefficient of the catalyst and calculated by taking a slope from the plot of $E_{p,c}$ *vs* ln ν ,[2] D_o = diffusion coefficient (cm^2/s), υ = scan rate (V/s).

From i_p *vs* square root of scan rate plot, eq (3) can remodified as

Slope $= 2.69 \times 10^5 A {n_p}^{1.5} [cat] \sqrt{D_0 \nu \alpha}$

$$D_0 = \left(\frac{slope}{2{\cdot}69 \times 10^5 A {n_p}^{1{\cdot}5} [cat] \sqrt{\alpha}} \right)^2$$

Here, A=0.07 cm^2, n_p = 2, [cat]=0.000001 mol/dm^3, α ≈ 0.4 (for **1**) and 0.3 (for **3**)

For HER: slope (Figure S6) = 77.8×10^{-6} **$D_0 = 5.3 \times 10^{-6}$ cm^2/s in MeOH**

For ligand: slope (Figure S7) = 128.3×10^{-6} **$D_0 = 19.3 \times 10^{-6}$ cm^2/s in MeOH**

HER equation for TOF calculation:

The relationship between the catalytic current (i_{cat}), catalyst concentration [cat], acid concentration [H^+], which is first order with respect to catalyst and second order with acid under scan rate independent condition[3-4] is mentioned in eq (4)

$$i_{cat} = n_{cat} F A [cat] \sqrt{Dk[H^+]^2} \qquad (4)$$

Where n_{cat} stands for number of electrons involved in catalysis.

After dividing eq (4) by the Randles-Ševčík equation:

$$\frac{j_{cat}}{j_p} = \frac{n_{cat} \times F}{2.69 \times 10^5 \, {n_p}^{1.5}} \sqrt{\frac{k[H^+]^2}{\nu}} \qquad (5)$$

Under Pseudo first-order condition,[5] k_{obs}=k[H^+]^2 therefore eq. (5) can be modified as

$$\frac{j_{cat}}{j_p} = \frac{n_{cat} \times F}{2.69 \times 10^5 \, n_p{}^{1.5}} \sqrt{\frac{k_{obs}}{v}} \qquad (6)$$

Or $TOF_{max}/k_{obs} = 7.77 \times \frac{n_p^3}{n_{cat}^2} \times \upsilon \times \left[\frac{j_{cat}}{j_p}\right]^2$ (7)

At 12 mM acetic acid concentration for **1**(current density was measured after background subtraction, see figure S8):

j_{cat}/j_p = 6300/1557 = 4.04 v= 2.0 V/s $\boldsymbol{k_{obs}}$**/TOF$_{max}$= 509 s^{-1}**

At 14 mM acetic acid concentration for ligand **3** (current density was measured after background subtraction, see figure S11C):

j_{cat}/j_p = 2289/1412. = 1.62 v= 0.6 V/s $\boldsymbol{k_{obs}}$**/TOF$_{max}$= 25 s^{-1}**

^{1}H NMR of **1**

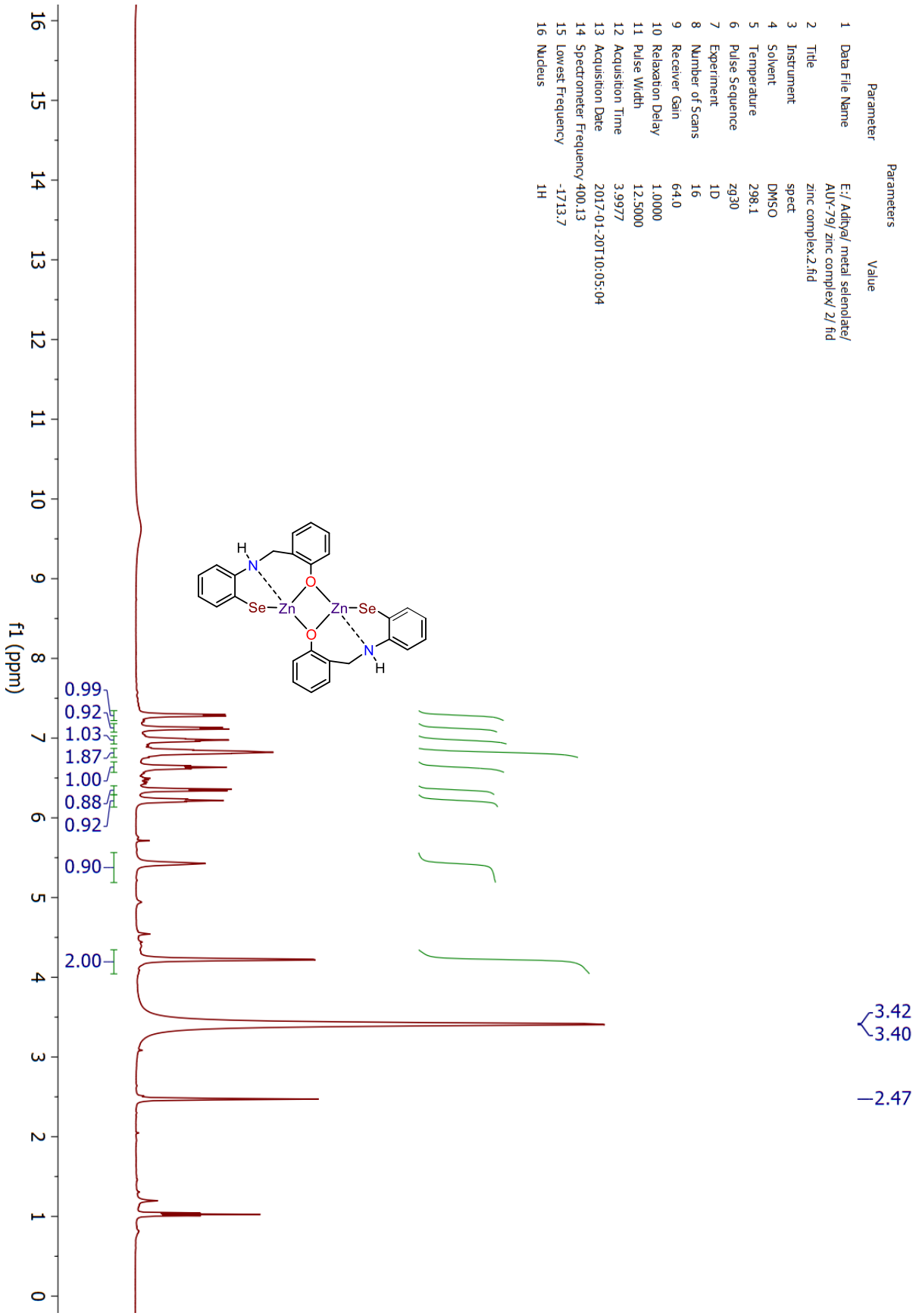
Parameters
Parameter Value
1 Data File Name E:/ Aditya/ metal selenolate/ AUY-79/ zinc complex/ 2/ fid
2 Title zinc complex2.fid
3 Instrument spect
4 Solvent DMSO
5 Temperature 298.1
6 Pulse Sequence zg30
7 Experiment 1D
8 Number of Scans 16
9 Receiver Gain 64.0
10 Relaxation Delay 1.0000
11 Pulse Width 12.5000
12 Acquisition Time 3.9977
13 Acquisition Date 2017-01-20T10:05:04
14 Spectrometer Frequency 400.13
15 Lowest Frequency -1713.7
16 Nucleus 1H
f1 (ppm)
0.99
0.92
1.03
1.87
1.00
0.88
0.92
0.90
2.00
3.42
3.40
2.47
H
N
Se
Zn
O
Zn
Se
N
H

^{13}C NMR of **1**

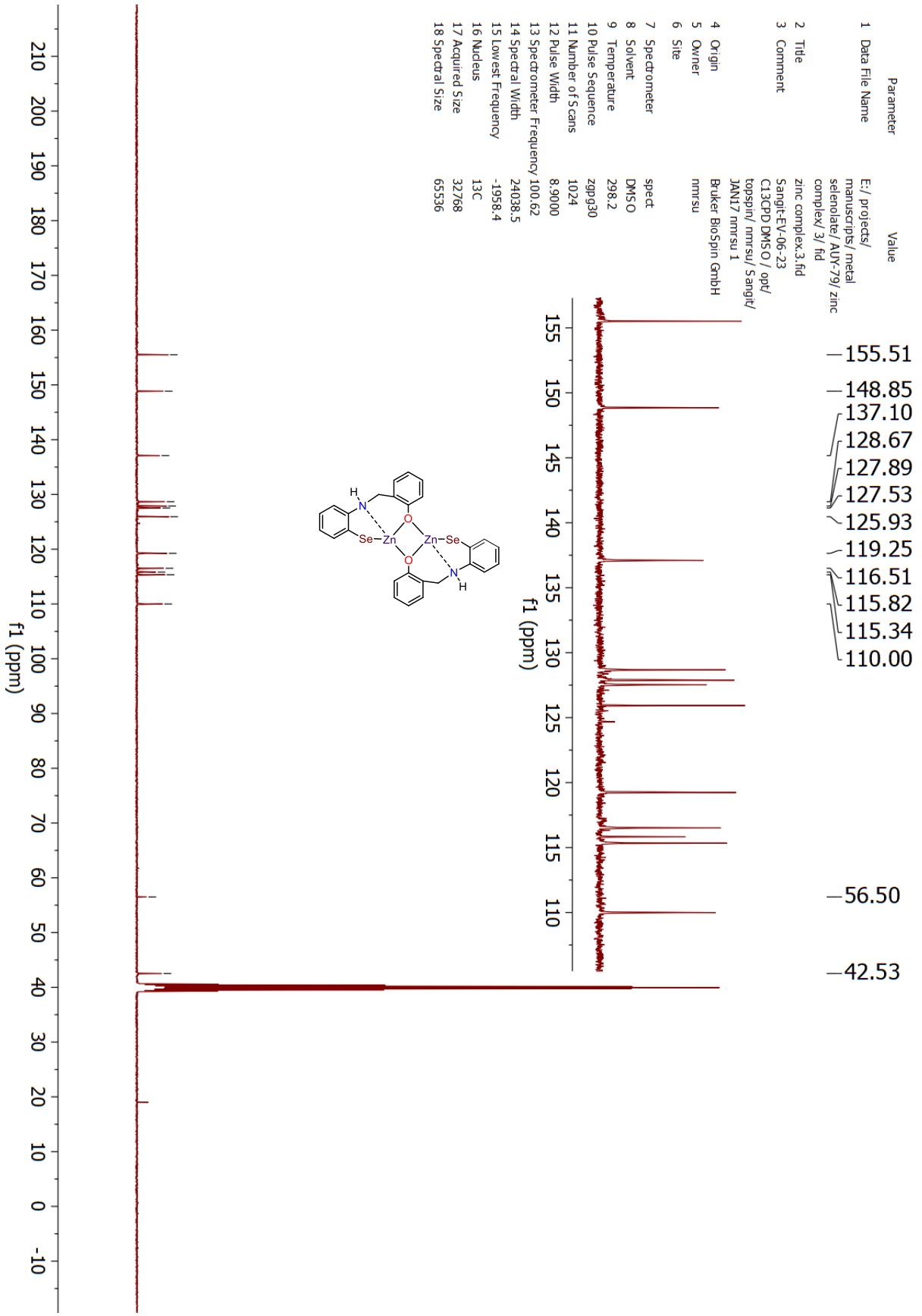
Parameter
Value
1 Data File Name
E:/ projects/ manuscripts/ metal selenolate/ AUY-79/ zinc complex/ 3/ fid
2 Title
zinc complex.3.fid
3 Comment
Sangit-EV-06-23 C13CPD DMSO / opt/ topspin/ nmrsu/ Sangit/ JAN17 nmrsu 1
4 Origin
Bruker BioSpin GmbH
5 Owner
nmrsu
6 Site
7 Spectrometer
spect
8 Solvent
DMSO
9 Temperature
298.2
10 Pulse Sequence
zgpg30
11 Number of Scans
1024
12 Pulse Width
8.9000
13 Spectrometer Frequency 100.62
14 Spectral Width
24038.5
15 Lowest Frequency
-1958.4
16 Nucleus
13C
17 Acquired Size
32768
18 Spectral Size
65536
155.51
148.85
137.10
128.67
127.89
127.53
125.93
119.25
116.51
115.82
115.34
110.00
56.50
42.53
f1 (ppm)
f1 (ppm)
H
N
O
Se
Zn
Zn
Se
O
N
H

^{77}Se NMR of **1**

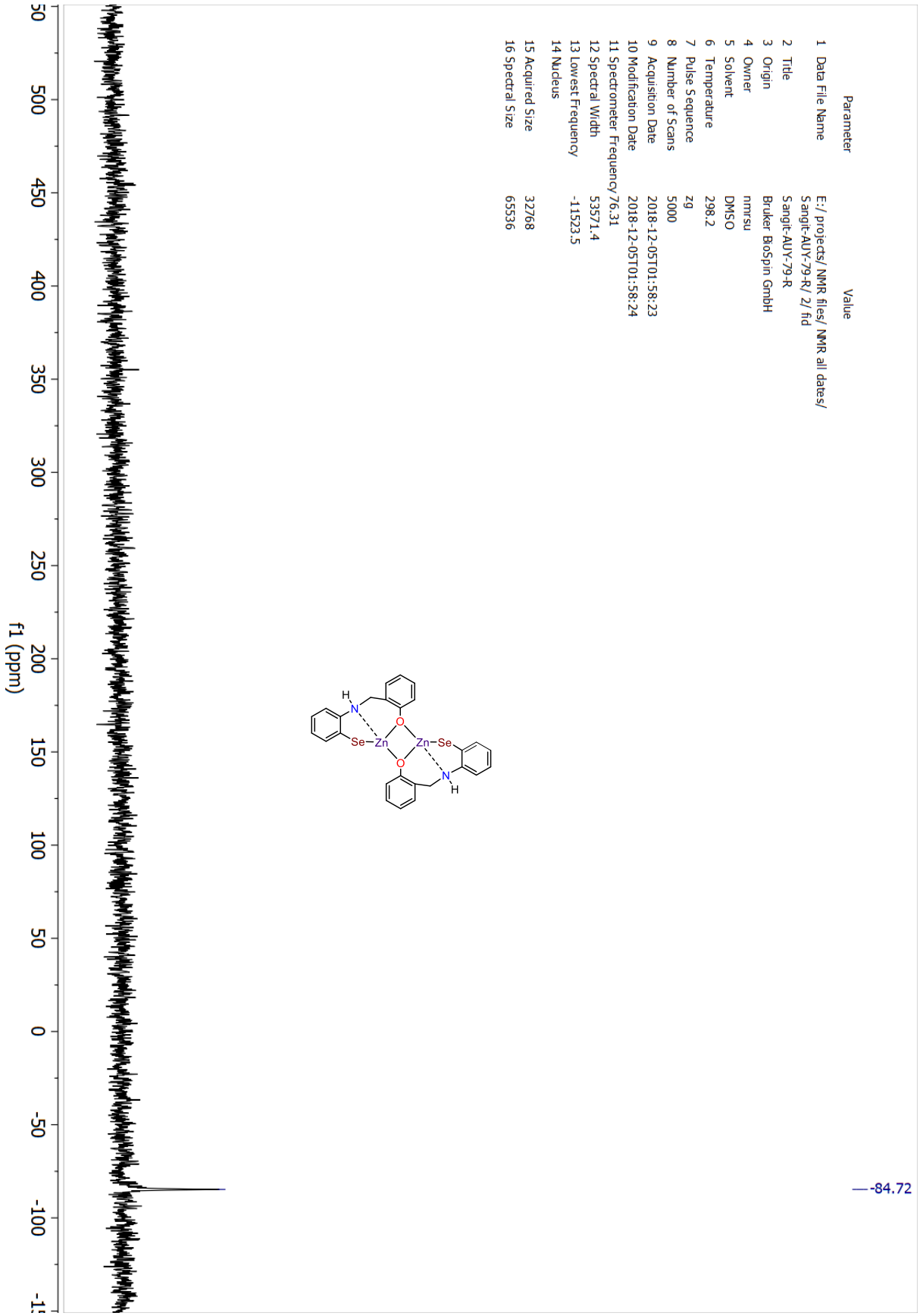
Parameter
Value
1 Data File Name
E:/ projects/ NMR files/ NMR all dates/ Sangit-AUY-79-R/ 2/ fid
2 Title
Sangit-AUY-79-R
3 Origin
Bruker BioSpin GmbH
4 Owner
nmrsu
5 Solvent
DMSO
6 Temperature
298.2
7 Pulse Sequence
zg
8 Number of Scans
5000
9 Acquisition Date
2018-12-05T01:58:23
10 Modification Date
2018-12-05T01:58:24
11 Spectrometer Frequency
76.31
12 Spectral Width
53571.4
13 Lowest Frequency
-11523.5
14 Nucleus
15 Acquired Size
32768
16 Spectral Size
65536
H
N
Se
Zn
O
Zn
Se
O
N
H
-84.72
f1 (ppm)
50
500
450
400
350
300
250
200
150
100
50
0
-50
-100

HRMS data of **1**

Display Report

Analysis Info

Acquisition Date	12/20/2018 12:28:09 PM		
Analysis Name	D:\Data\NEW USER DATA 2017\2018\DECEMBER\19 DEC\Dr S Kumar-AUY-79-R.d		
Method	tune_low_APCI.m	Operator	RUCHI
Sample Name	AUY-79-R	Instrument	micrOTOF-Q II 10330
Comment			

Acquisition Parameter

Source Type	APCI	Ion Polarity	Positive	Set Nebulizer	2.5 Bar
Focus	Not active	Set Capillary	4500 V	Set Dry Heater	200 °C
Scan Begin	50 m/z	Set End Plate Offset	-500 V	Set Dry Gas	4.0 l/min
Scan End	3000 m/z	Set Collision Cell RF	300.0 Vpp	Set Divert Valve	Waste

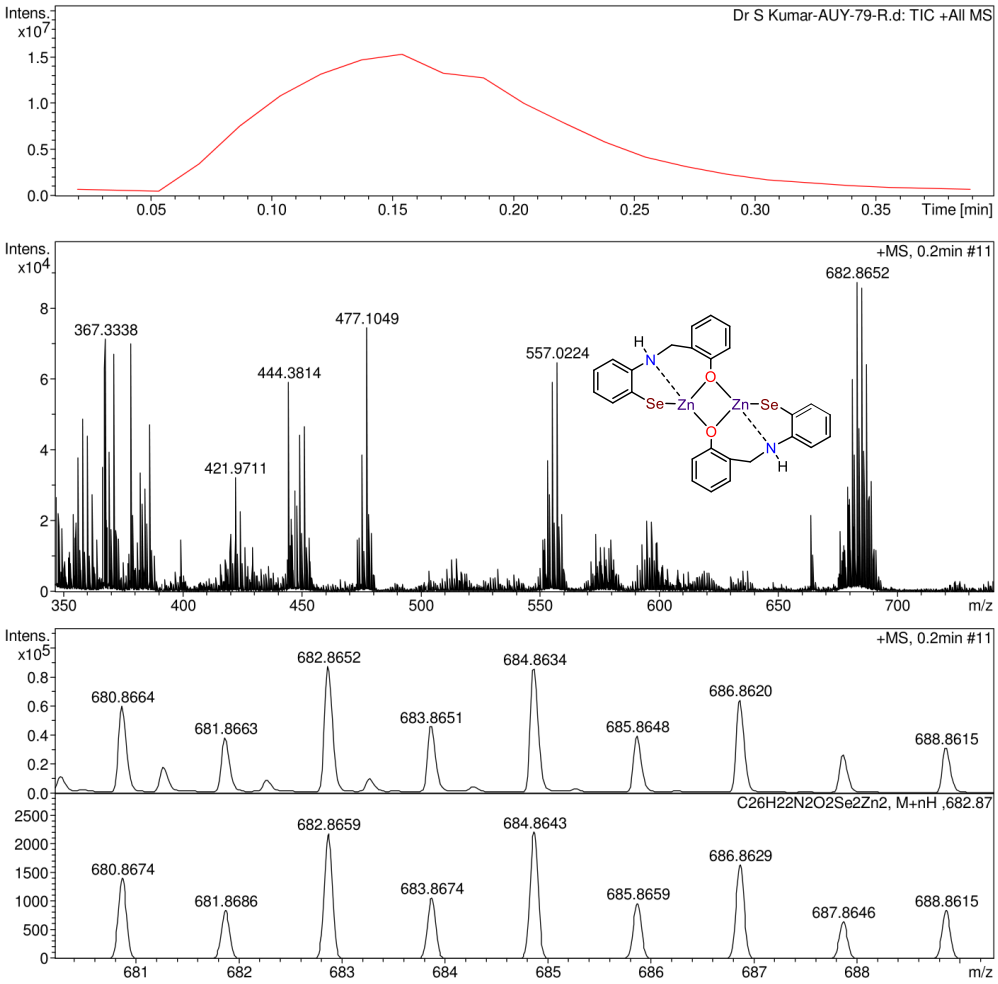

Bruker Compass DataAnalysis 4.0 printed: 12/20/2018 12:29:47 PM Page 1 of 1

1H NMR of **4**

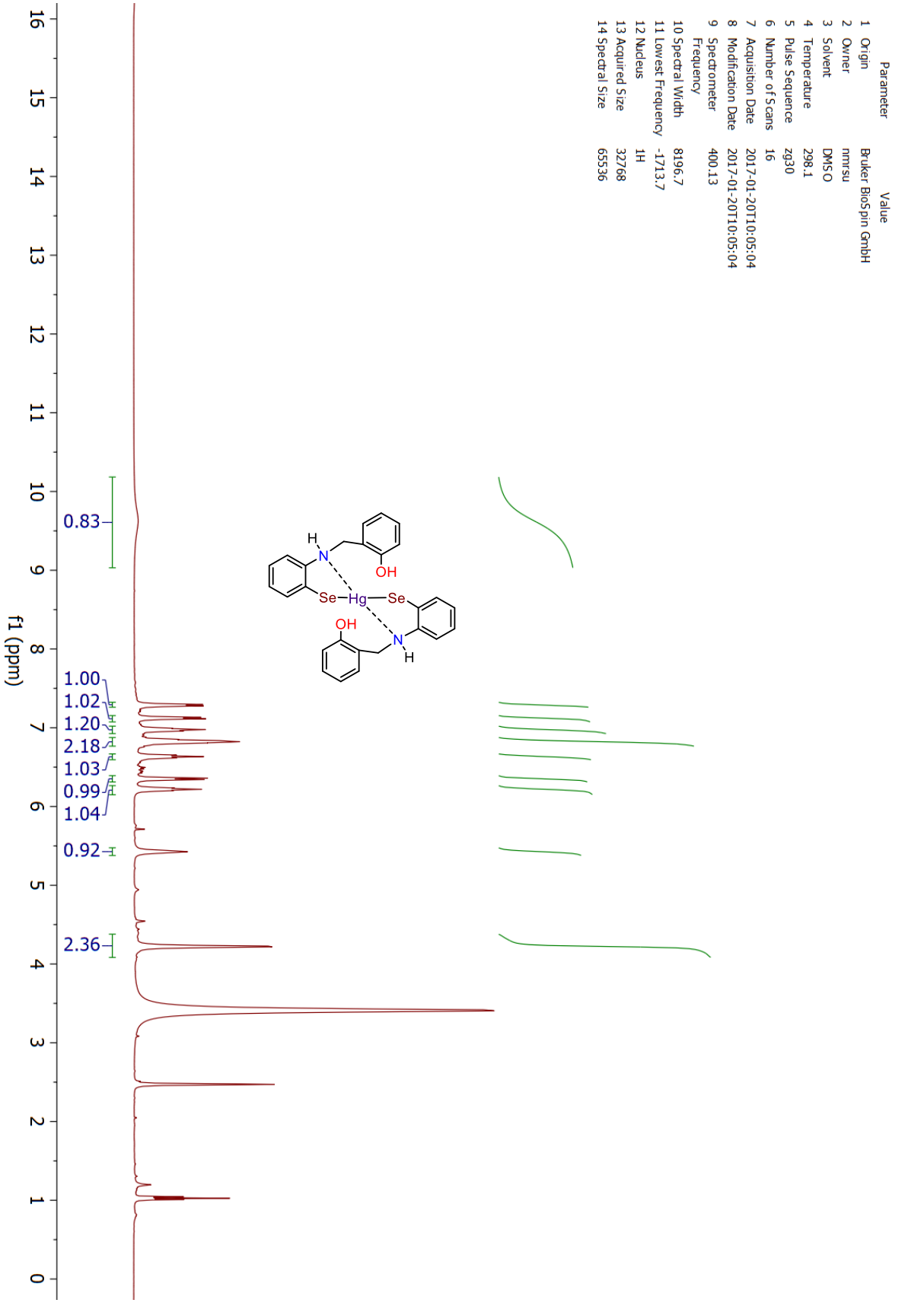
Parameter Value
1 Origin Bruker BioSpin GmbH
2 Owner nmrsu
3 Solvent DMSO
4 Temperature 298.1
5 Pulse Sequence zg30
6 Number of Scans 16
7 Acquisition Date 2017-01-20T10:05:04
8 Modification Date 2017-01-20T10:05:04
9 Spectrometer Frequency 400.13
10 Spectral Width 8196.7
11 Lowest Frequency -1713.7
12 Nucleus 1H
13 Acquired Size 32768
14 Spectral Size 65536
0.83
1.00
1.02
1.20
2.18
1.03
0.99
1.04
0.92
2.36
f1 (ppm)
H
N
OH
Se
Hg
Se
OH
N
H

^{13}C NMR of **4**

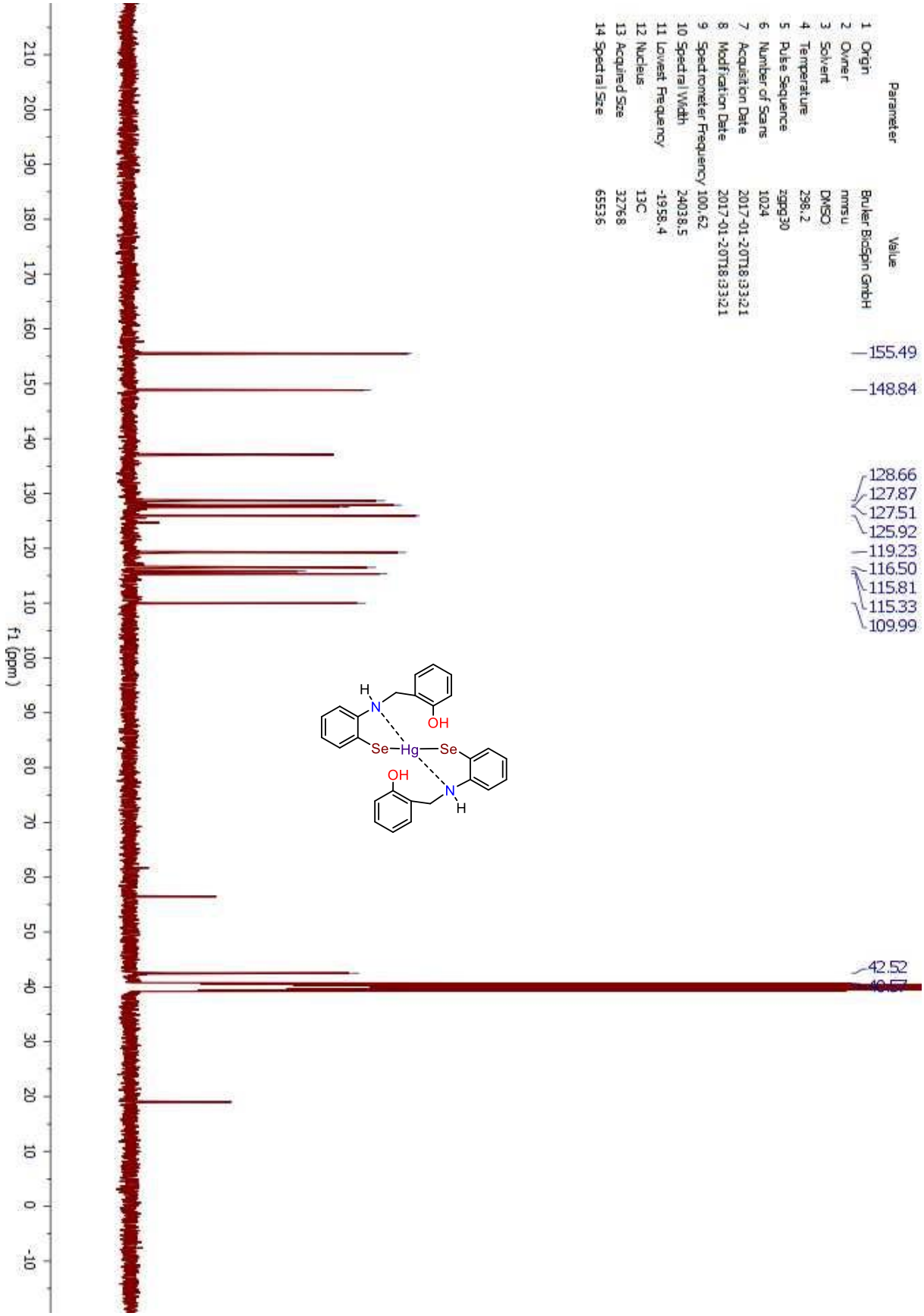
Parameter
Value
1 Origin
Bruker BioSpin GmbH
2 Owner
nmrsu
3 Solvent
DMSO
4 Temperature
298.2
5 Pulse Sequence
zgpg30
6 Number of Scans
1024
7 Acquisition Date
2017-01-20T18:33:21
8 Modification Date
2017-01-20T18:33:21
9 Spectrometer Frequency
100.62
10 Spectral Width
24038.5
11 Lowest Frequency
-1958.4
12 Nucleus
13C
13 Acquired Size
32768
14 Spectral Size
65536
155.49
148.84
128.66
127.87
127.51
125.92
119.23
116.50
115.81
115.33
109.99
42.52
f1 (ppm)
H
N
OH
Se
Hg
Se
OH
N
H

^{77}Se NMR of **4**

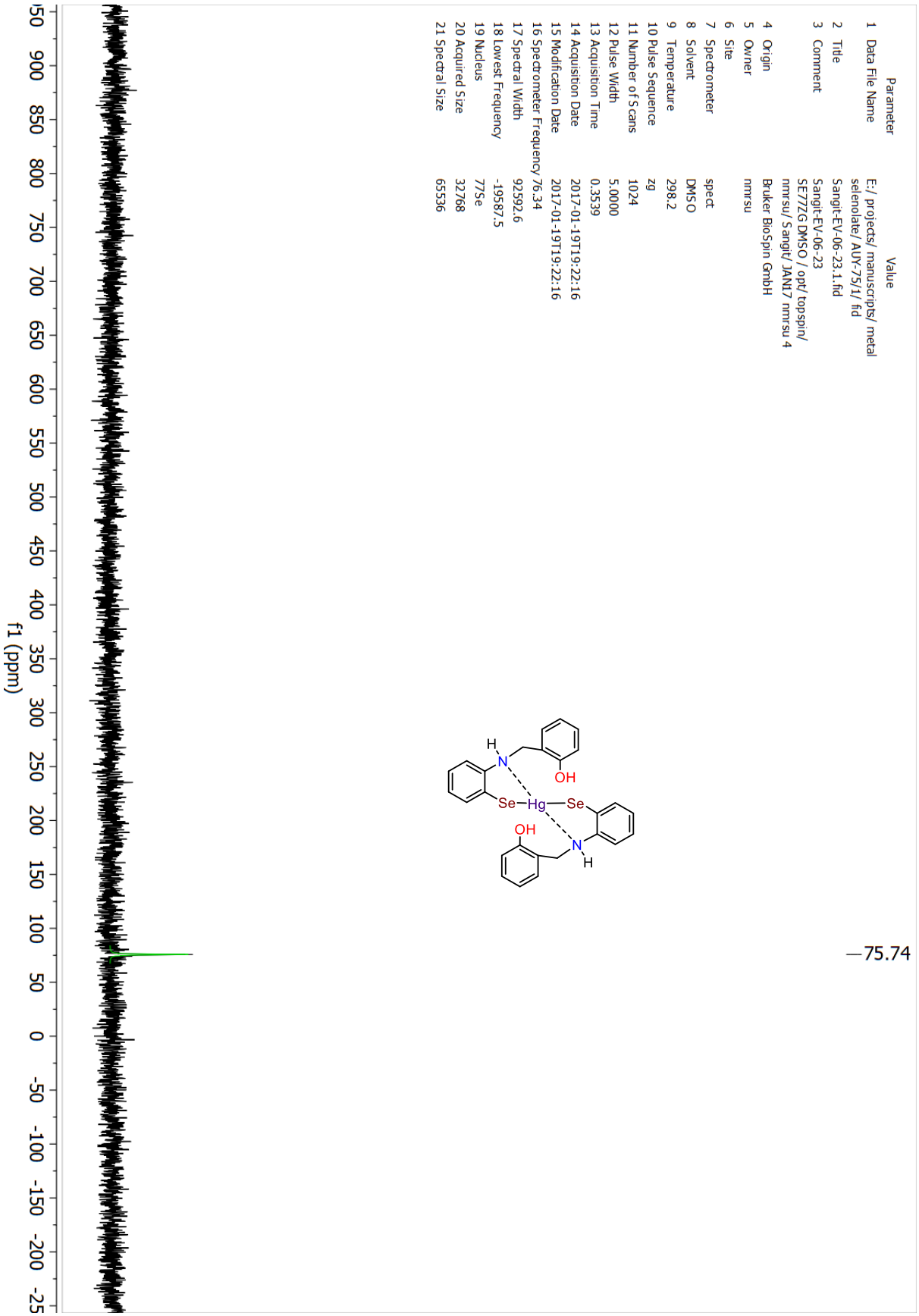
Parameter
Value
1 Data File Name
E:/ projects/ manuscripts/ metal selenolate/ AUY-75/1/ fid
2 Title
Sangit-EV-06-23.1.fid
3 Comment
Sangit-EV-06-23
SE77ZG DMSO / opt/ topspin/ nmrsu/ Sangit/ JAN17 nmrsu 4
4 Origin
Bruker BioSpin GmbH
5 Owner
nmrsu
6 Site
7 Spectrometer
spect
8 Solvent
DMSO
9 Temperature
298.2
10 Pulse Sequence
zg
11 Number of Scans
1024
12 Pulse Width
5.0000
13 Acquisition Time
0.3539
14 Acquisition Date
2017-01-19T19:22:16
15 Modification Date
2017-01-19T19:22:16
16 Spectrometer Frequency/76.34
17 Spectral Width
92592.6
18 Lowest Frequency
-19587.5
19 Nucleus
77Se
20 Acquired Size
32768
21 Spectral Size
65536
H
N
OH
Se
Hg
Se
OH
N
H
−75.74
f1 (ppm)
150
900
850
800
750
700
650
600
550
500
450
400
350
300
250
200
150
100
50
0
-50
-100
-150
-200
-25

HRMS data of **4**

Display Report

Analysis Info

Analysis Name	D:\Data\NEW USER DATA 2017\2019\JAN\10 jan\Prof.S.Kumar-AUY-75.d	Acquisition Date	1/10/2019 3:16:42 PM
Method	tune_wide _APCI_23.06.m	Operator	RUCHI
Sample Name	AUY-75	Instrument	micrOTOF-Q II 10330
Comment			

Acquisition Parameter

Source Type	APCI	Ion Polarity	Positive	Set Nebulizer	2.5 Bar
Focus	Not active	Set Capillary	4000 V	Set Dry Heater	200 °C
Scan Begin	50 m/z	Set End Plate Offset	-500 V	Set Dry Gas	4.0 l/min
Scan End	3000 m/z	Set Collision Cell RF	600.0 Vpp	Set Divert Valve	Waste

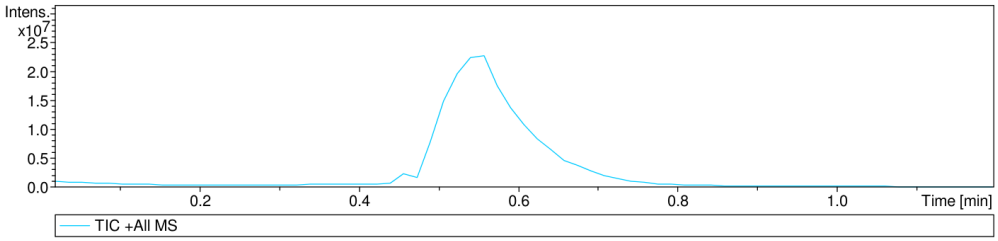

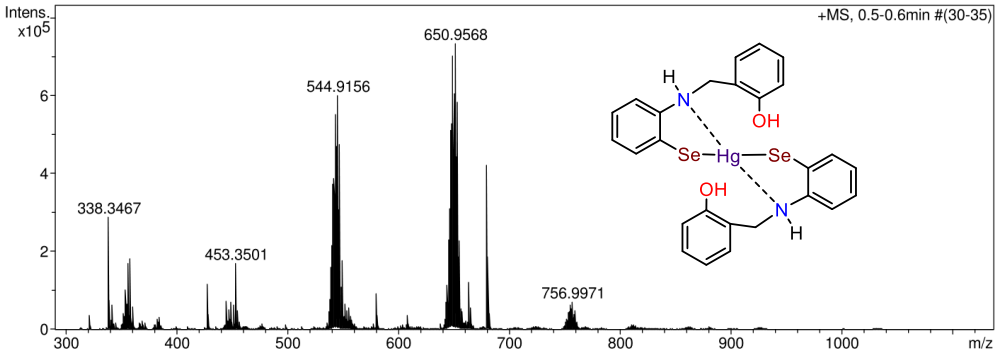

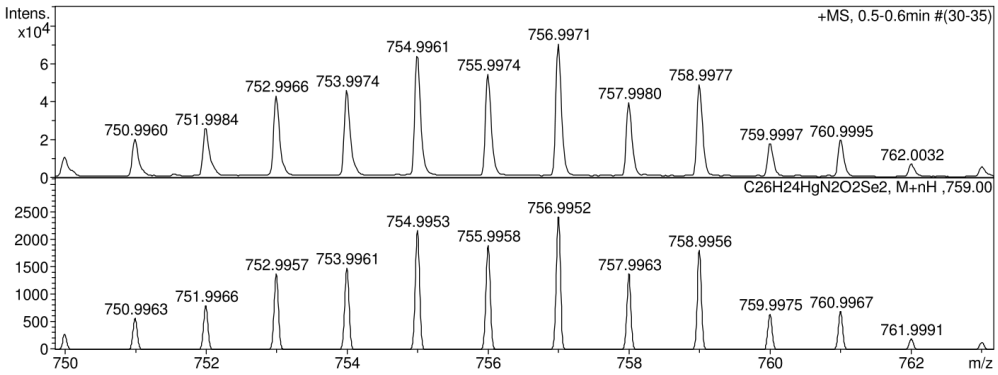

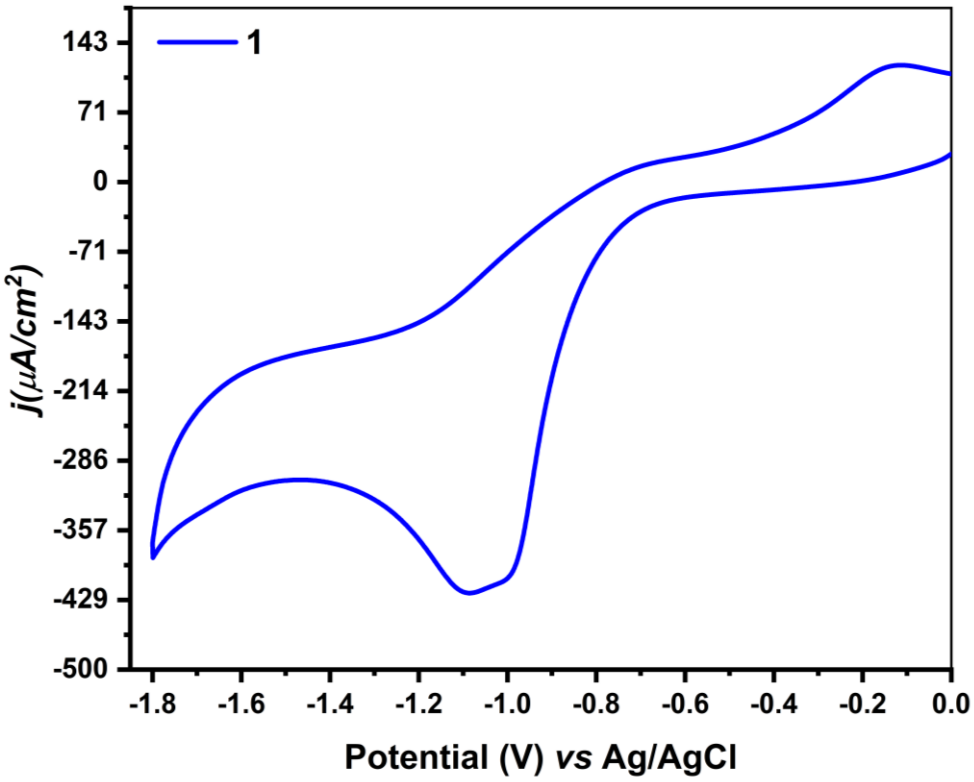

Figure S1. Cyclic voltammogram (CV) of zinc selenolate **1** (1mM) in acetonitrile solvent under cathodic potential at 0.1V/s scan rate using 0.1 M $^{n}Bu_4NPF_6$ supporting electrolyte.

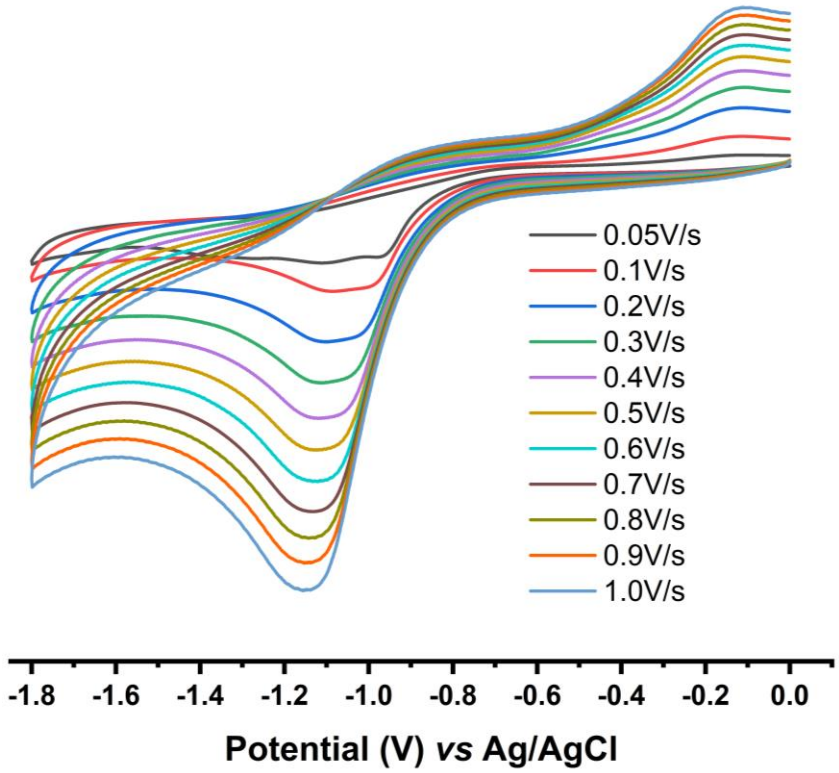

Figure S2. CV of bimetallic zinc selenolate **1** at various scan rate in acetonitrile.

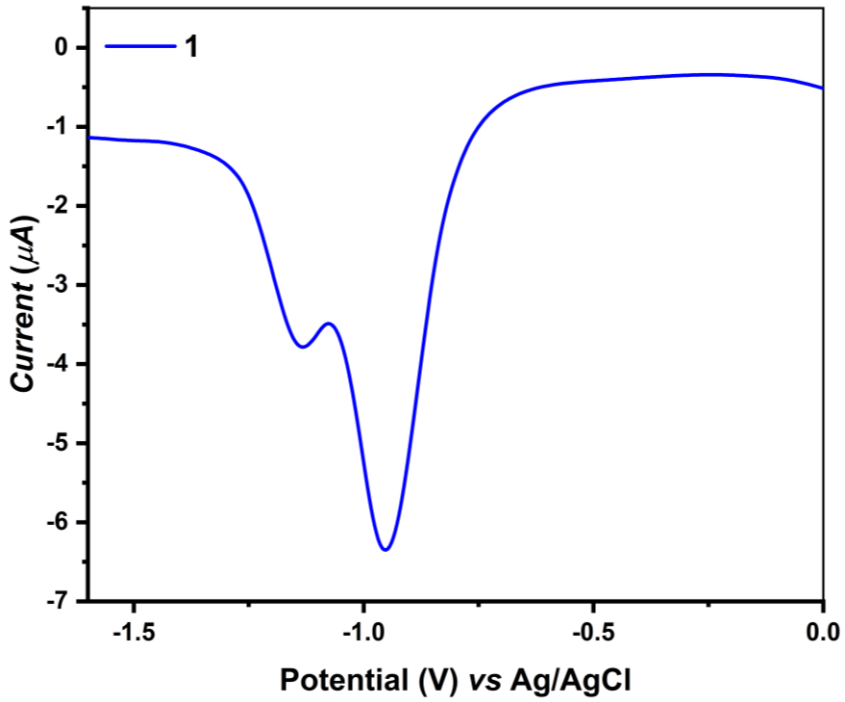

Figure S3. Differential Pulse Voltammetry graph of bimetallic zinc selenolate in acetonitrile. These graphs confirm the two-electron transfer in the zinc selenolate electrocatalyst under cathodic potential.

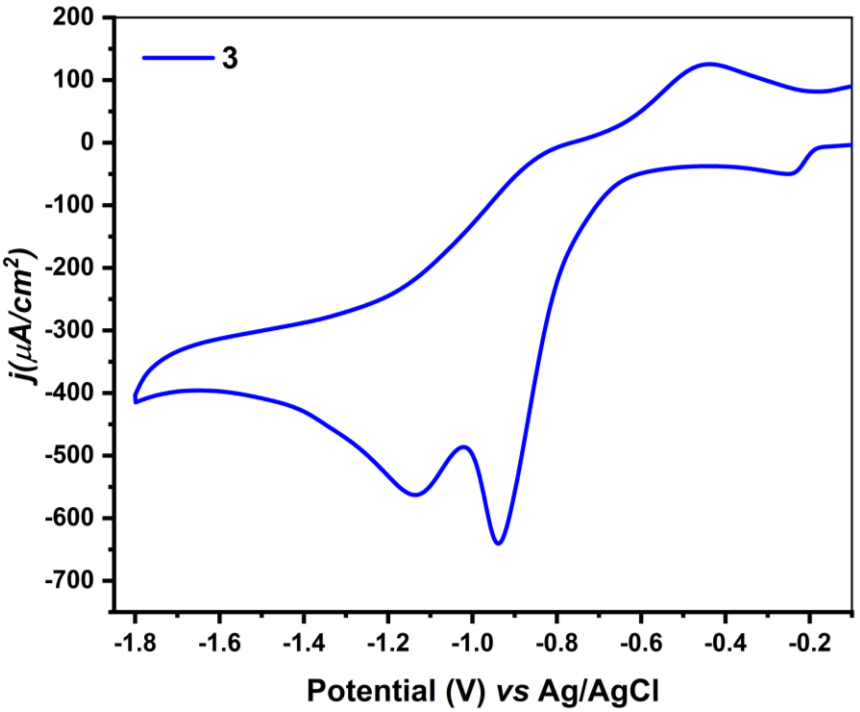

Figure S4. CV characterization of diselenide ligand **3** (1mM) in acetonitrile solvent using 0.1M $^{n}Bu_4NPF_6$ as supporting electrolyte.

CV of zinc selenolate 1 at different scan rate in methanol

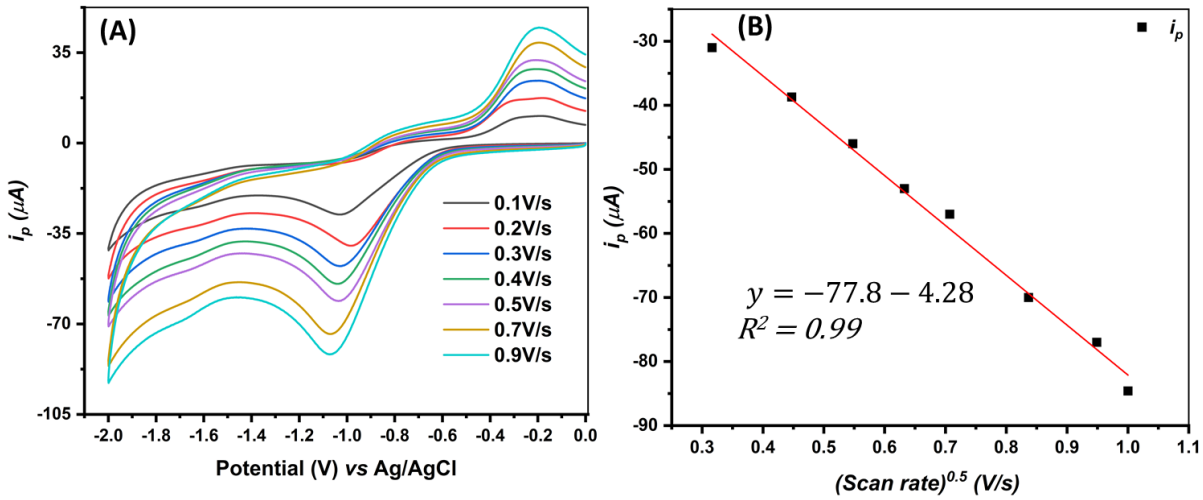

Figure S5 A-B. (A) Cyclic Voltammogram of bimetallic zinc selenolate **1** (1mM) using 0.1M $^{n}Bu_4NPF_6$ as supporting electrolyte in methanol solution at varying scan rates. **(B)** Corresponding linear plot (for HER) of i_p *vs* $\nu^{0.5}$.

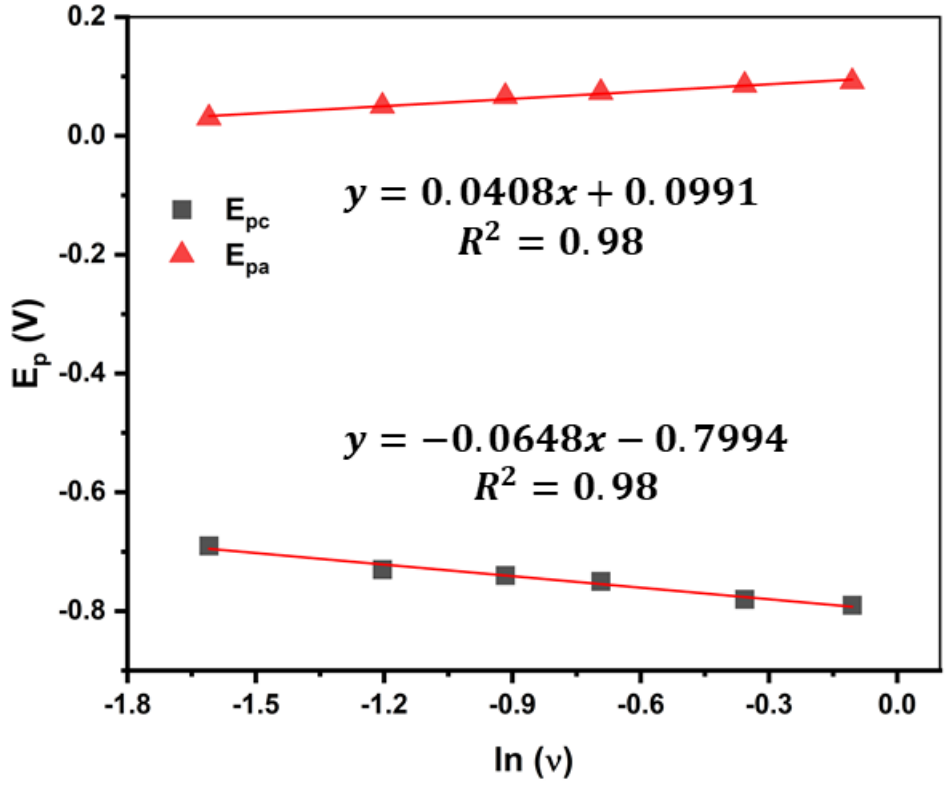

Figure S6. Plot of peak potential (E_p) *vs* ln(ν) for bimetallic zinc selenolate **1** in methanol solvent at room temperature.

CV of diselenide ligand 3 at different scan rate in methanol

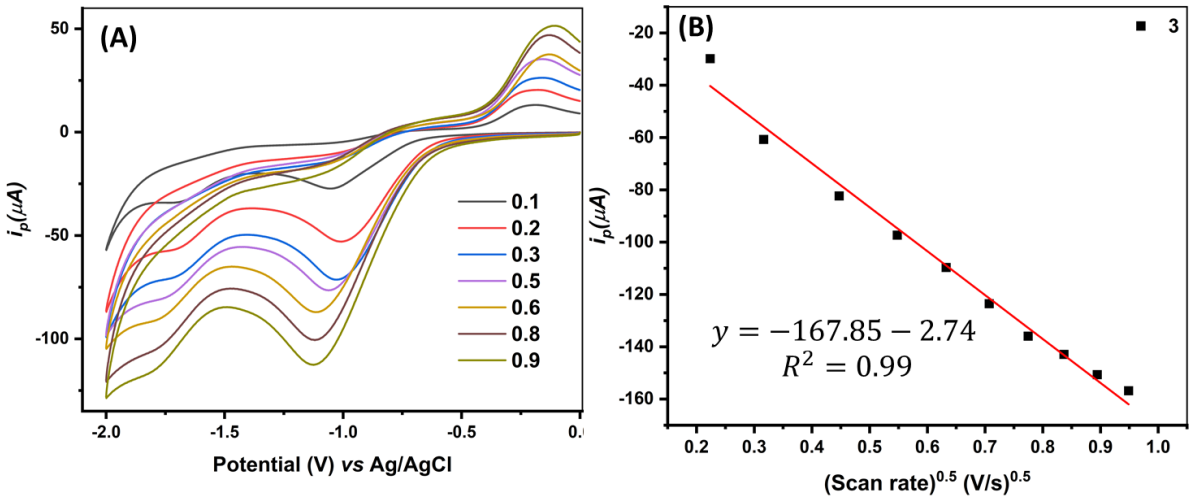

Figure S7 A-B. (A) Cyclic Voltammogram of diselenide ligand **3** (1mM) using 0.1M $^{n}Bu_4NPF_6$ as supporting electrolyte in methanol solution at varying scan rates from 0.1 V/s to 1.0 V/s. **(B)** Corresponding linear plot (for HER) of i_p *vs* $\nu^{0.5}$.

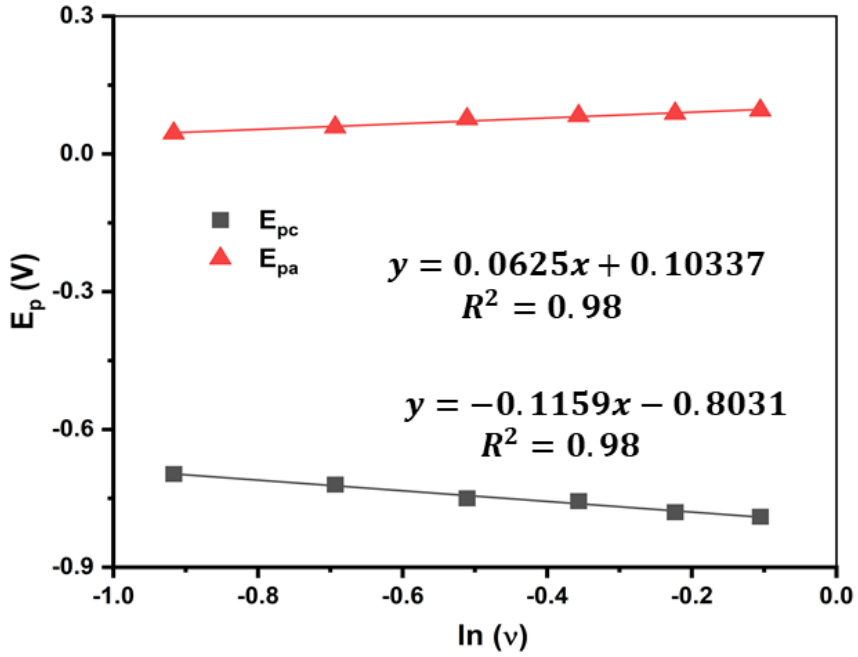

Figure S8. Plot of peak potential (E_p) *vs* ln(ν) for diselenide ligand **3** in methanol solvent at room temperature.

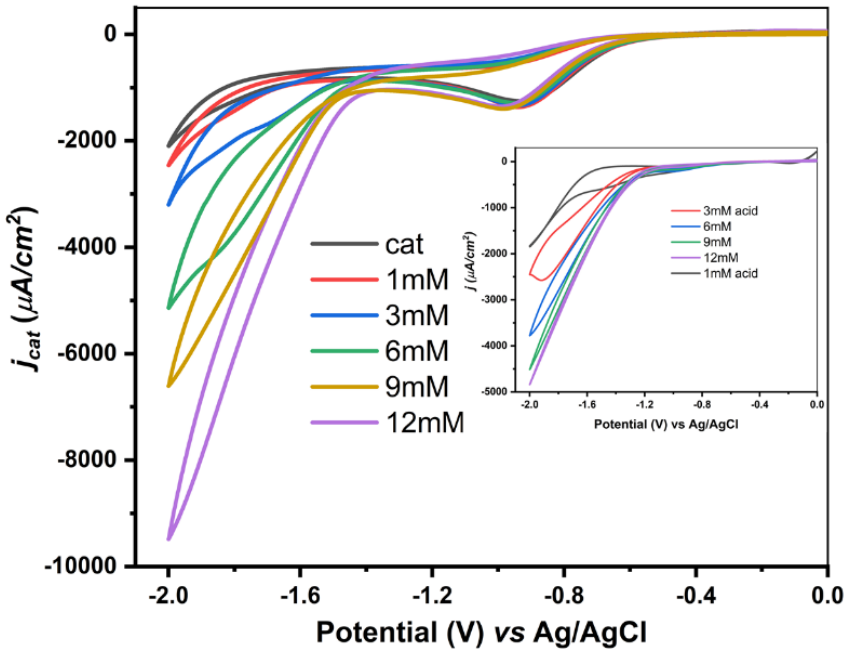

Figure S9. Electrochemical H_2 evolution with the addition of acetic acid by catalyst **1** (1 mM) using $^{n}Bu_4NPF_6$(0.1 M) as a supporting electrolyte in methanol solvent at 0.05V/s scan rate (HER in methanol without catalyst shown in the inset of the graph).

Tafel Analysis of HER for zinc selenolate 1

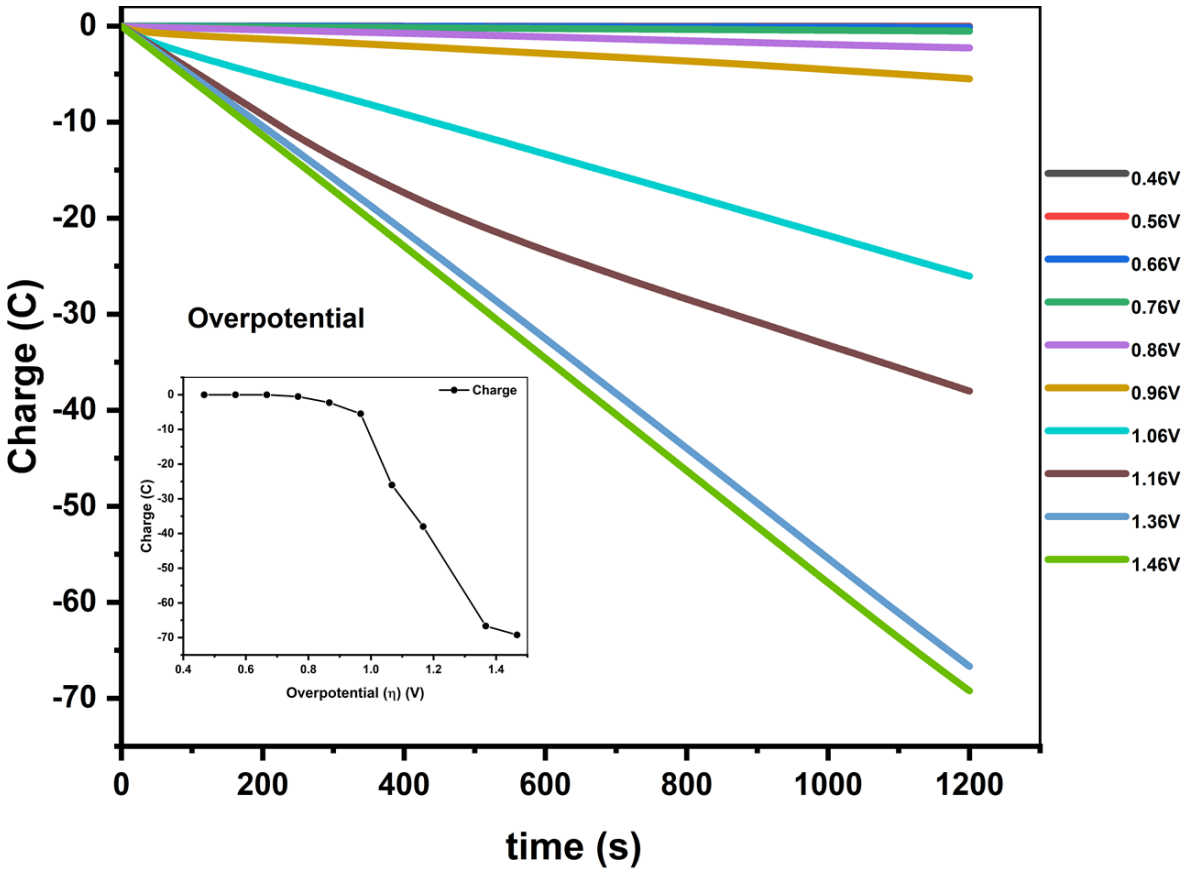

Figure S10. Tafel analysis for HER by zinc selenolate catalyst **1.** The actual overpotential of this complex was determined by controlled potential electrolysis at different potentials using mercury pool as the working electrode in methanol with acetic acid. The overpotentials were applied over a period of 1200 s and altered from 0.46 to 1.46 V *vs* Ag/AgCl. The total consumption of charge was negligible below 0.86 V *vs* Ag/AgCl, whereas at more negative potentials the charge increased linearly over time. Moreover, the charge *vs* overpotential plot (Figure S7 inset) clearly indicates the consumption of charge started increasing consistently after an overpotential of 0.86 V *vs* Ag/AgCl concomitant with the generation of bubbles. Therefore, the onset and actual overpotentials reside at close proximity.

HER at different scan rate in methanol by zinc selenolate complex 1

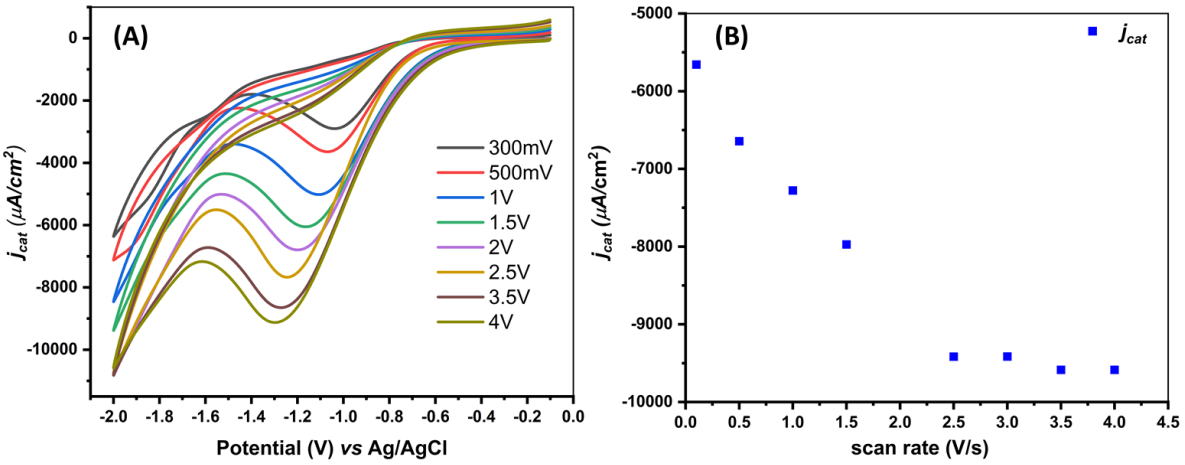

Figure S11 A-B. **(A)** Cyclic Voltammogram of bimetallic zinc selenolate **1** (1mM) using 0.1M $^{n}Bu_4NPF_6$ as supporting electrolyte in MeOH solution with varying the scan rate at 12mM acid concentration. **(B)** Corresponding linear plot for the j_{cat} (µA/cm^2) *vs* scan rate (V/s)

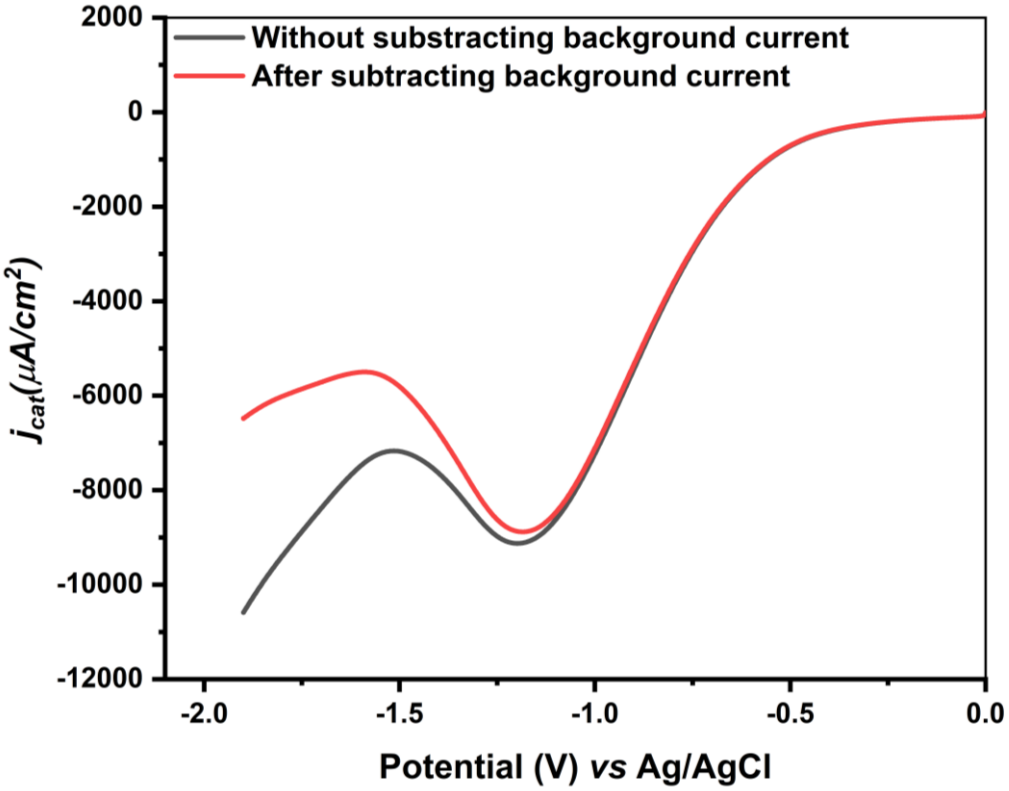

Figure S11 C. LSV of **1** (1mM) at under saturated acid concentration i.e., 12mM and saturated scan rate (2.0 V/s) with (Red line) and without (Black line) subtracting the background current.

CV of 1 at various concentration in MeOH

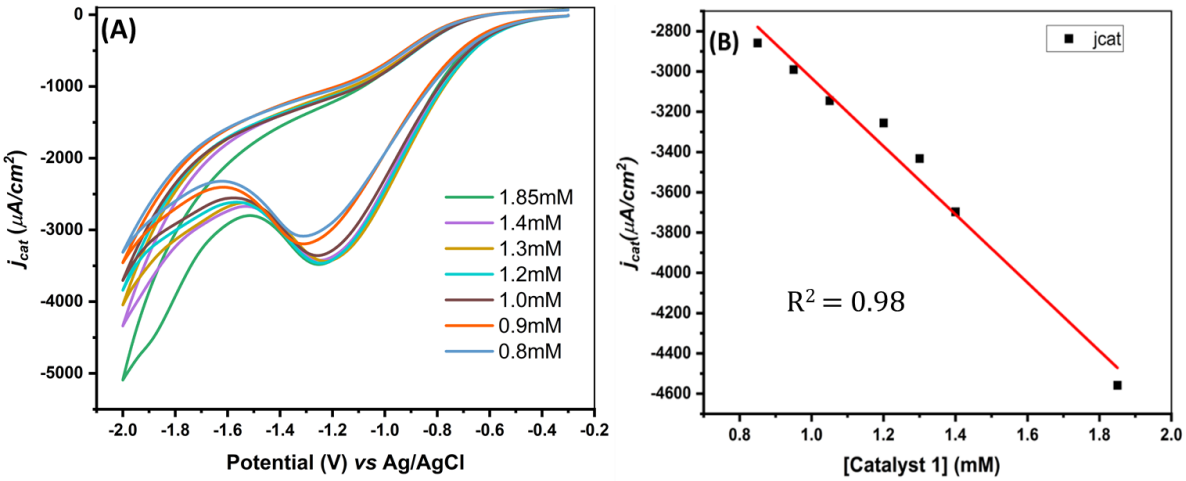

Figure S12 A-B. (A) CV of catalyst **1** at different concentration (0.1 M ^{n}Bu$_4$NPF$_6$) in the presence of 12mM acetic acid concentration under cathodic direction. **(B)** j_{cat} *vs* [catalyst **1**] graph under cathodic direction at 0.5 V/s.

CV of diselenide ligand 3 at various acid concentration in MeOH

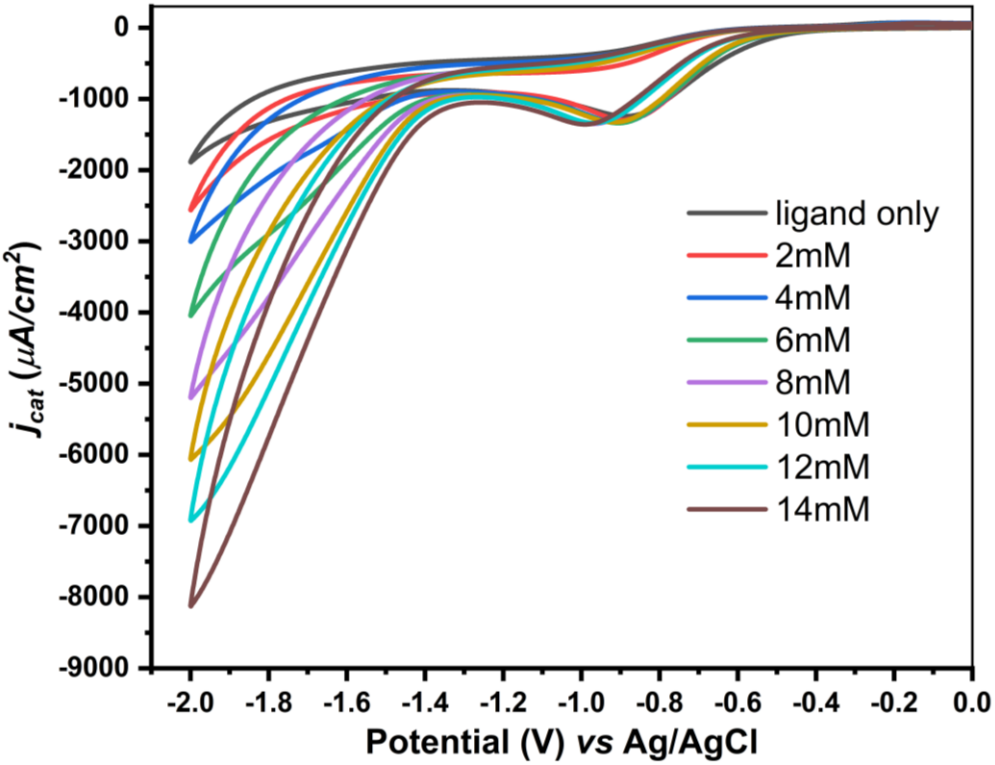

Figure S13. CV graph for the HER by diselenide ligand **3** at 0.05 V/s scan rate in various concentration of acetic acid in methanol solvent ($^{n}Bu_4NPF_6$ as a supporting electrolyte).

HER at different scan rate in methanol by diselenide ligand 3

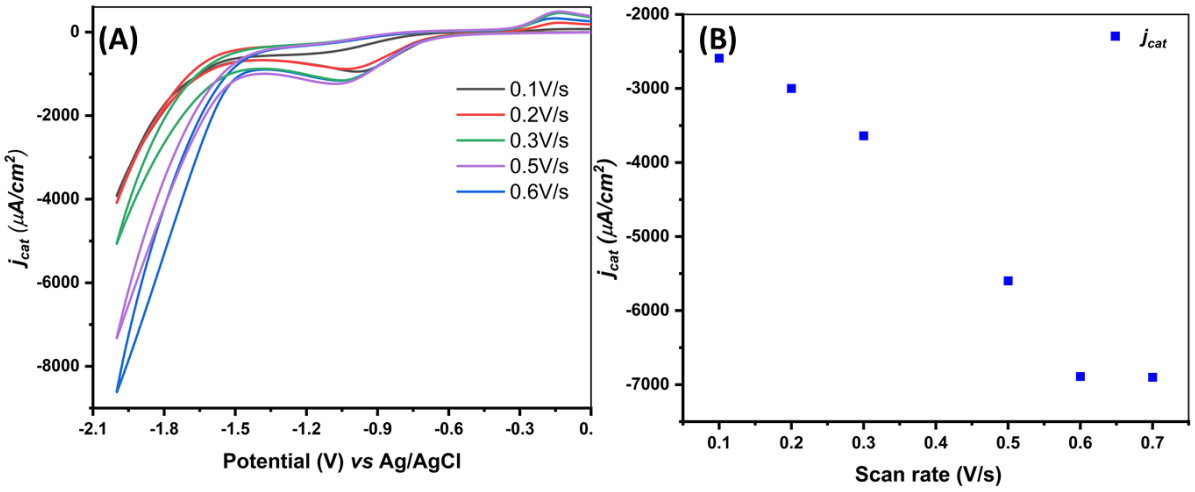

Figure S14 A-B. **(A)** Cyclic Voltammogram of aminophenolic diselenide ligand **3** (1mM) at 14mM acetic acid concentration using 0.1M $^{n}Bu_4NPF_6$ as supporting electrolyte in MeOH solution with varying the scan rate. **(B)** Corresponding linear plot for the j_{cat} (µA/cm^2) *vs* scan rate (V/s) for the **1** (1mM) and 14mM acid concentration.

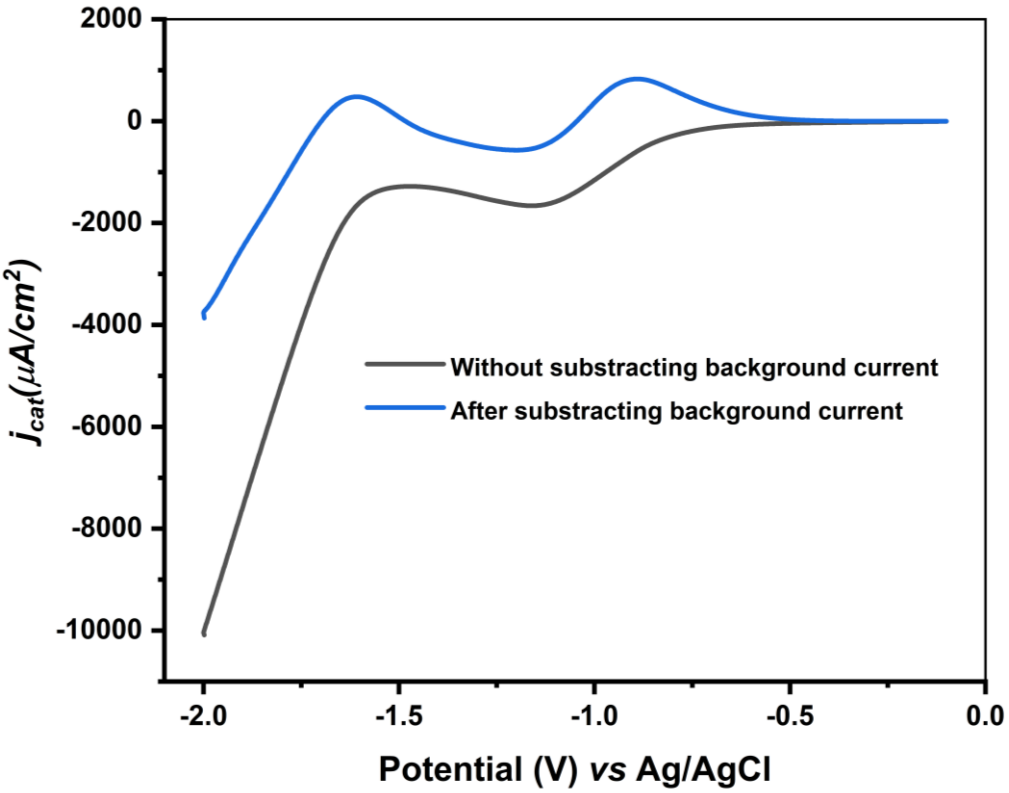

Figure S14 C. LSV of **3** (1mM) at under saturated acid concentration i.e., 14mM and saturated scan rate (0.6 V/s) with (Blue line) and without (Black line) subtracting the background current.

CV of $ZnCl_2$

The CV study of $ZnCl_2$ was done in ethanol due to the insolubility of $ZnCl_2$ in propylene carbonate.

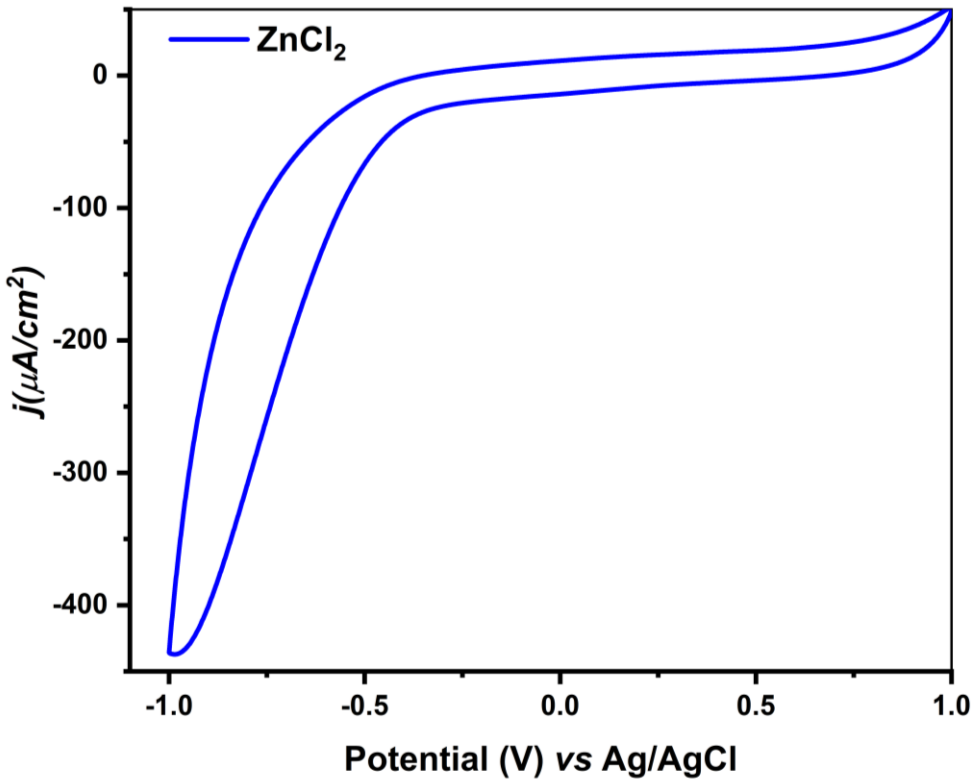

Figure S15. Cyclic Voltammogram of $ZnCl_2$ (1mM) in ethanol solution using $^{n}Bu_4NPF_6$, as $ZnCl_2$ is not soluble in propylene carbonate.

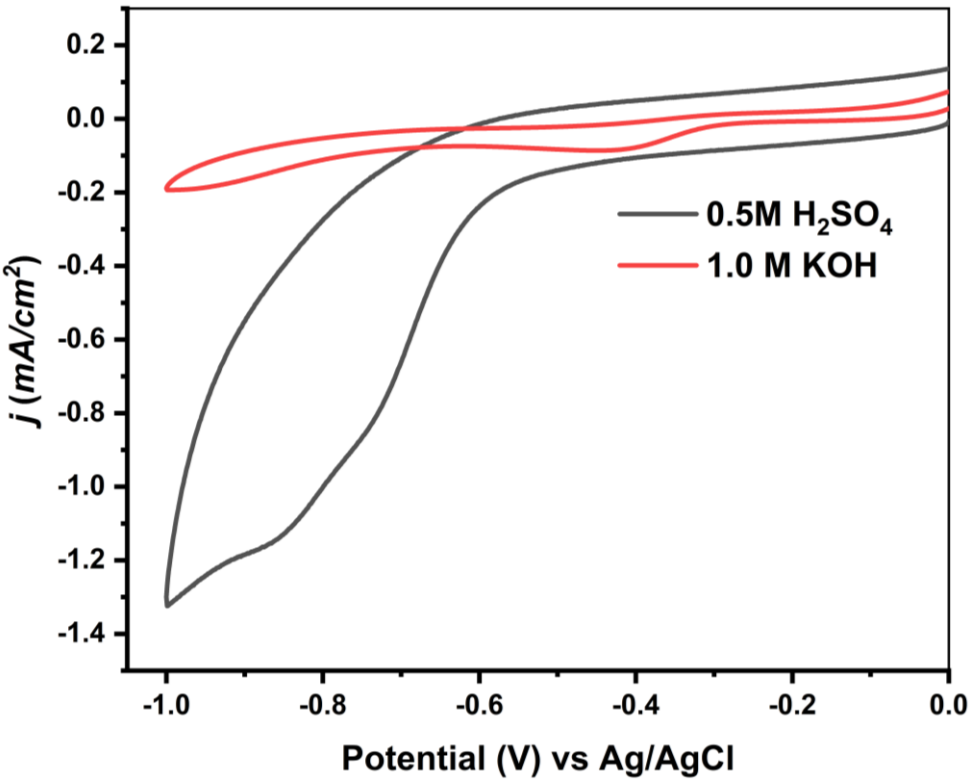

Figure S16. Current density comparison for the HER in 0.5 M H_2SO_4 (Black line) and 1.0M KOH (Red Line) under heterogeneous condition.

Constant Potential Electrolysis

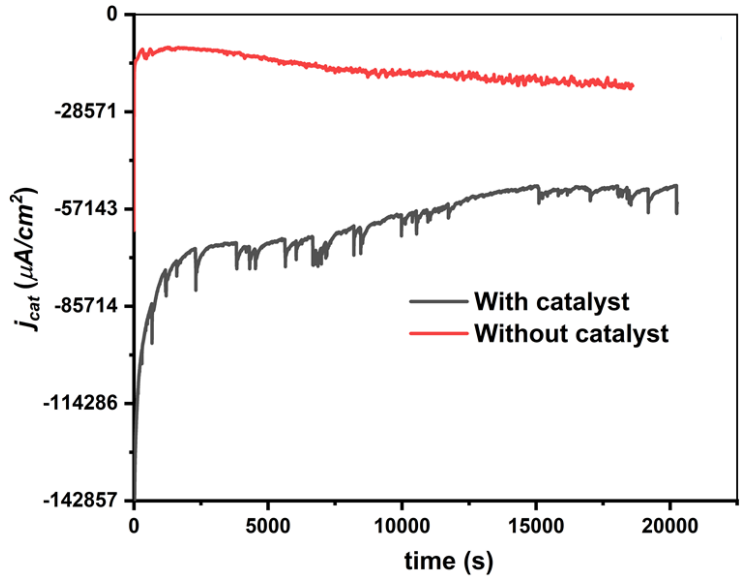

Figures S17. Constant potential electrolysis for HER at -1.78 V *vs* Ag/AgCl of catalyst **1** (5mM) in methanol using 0.1M $^{n}Bu_4NPF_6$ as supporting electrolyte. The spikes in currents are due to the formation of hydrogen gas bubbles.

Post electrolysis analysis

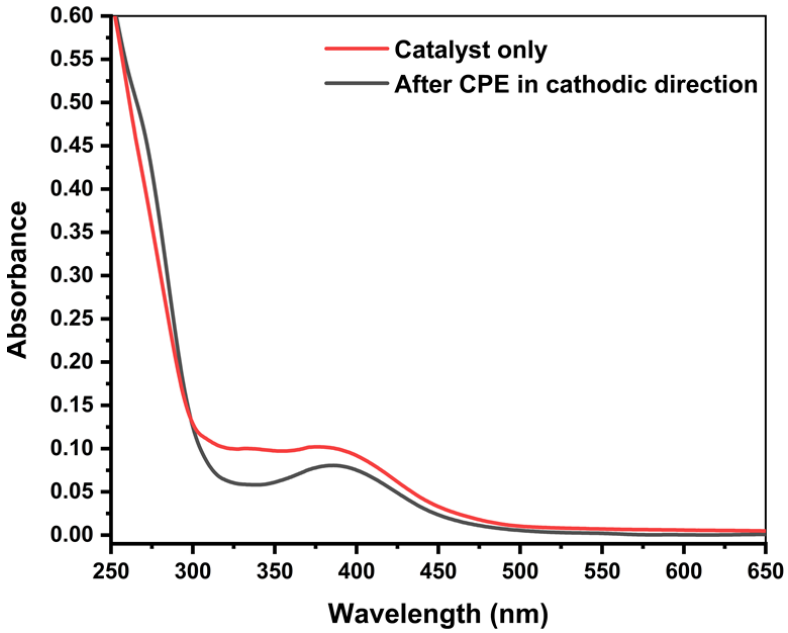

Figure S18. UV-Visible spectra of the reaction mixture after CPE under cathodic potential in methanol solvent, using 1mM zinc selenolate catalyst **1** and $^{n}Bu_4NPF_6$ (0.1 M) as a supporting electrolyte.

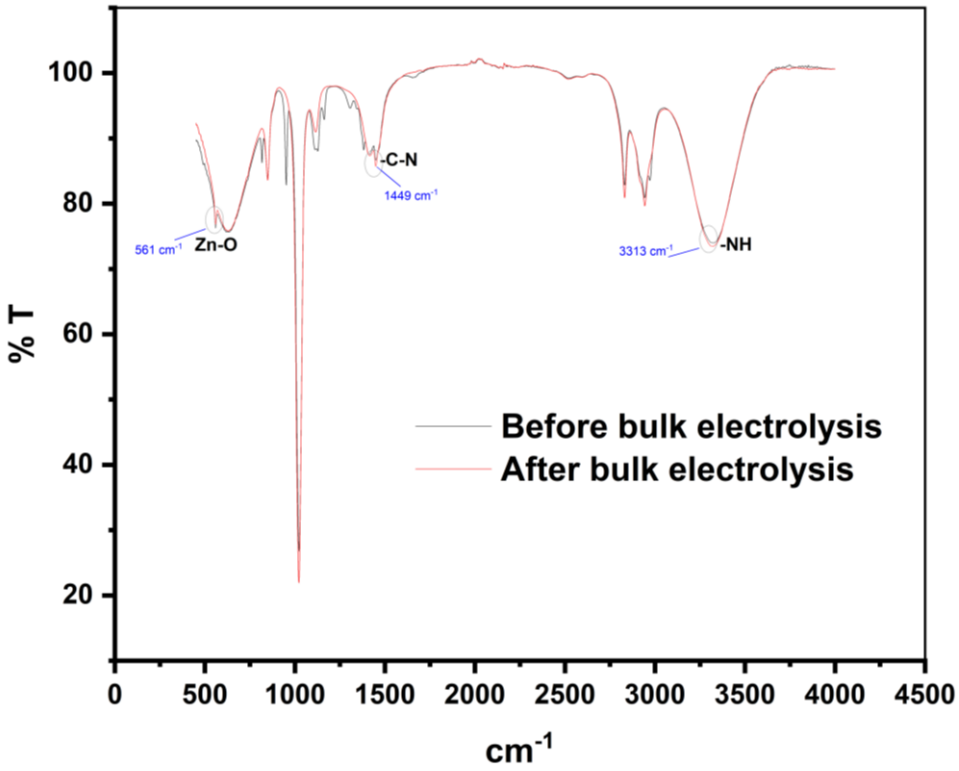

Figure S19. IR spectra of **1** before (upper one) and after (lower one) the bulk electrolysis solution in methanol containing 12mM acid at -1.78 V *vs* Ag/AgCl under cathodic potential.

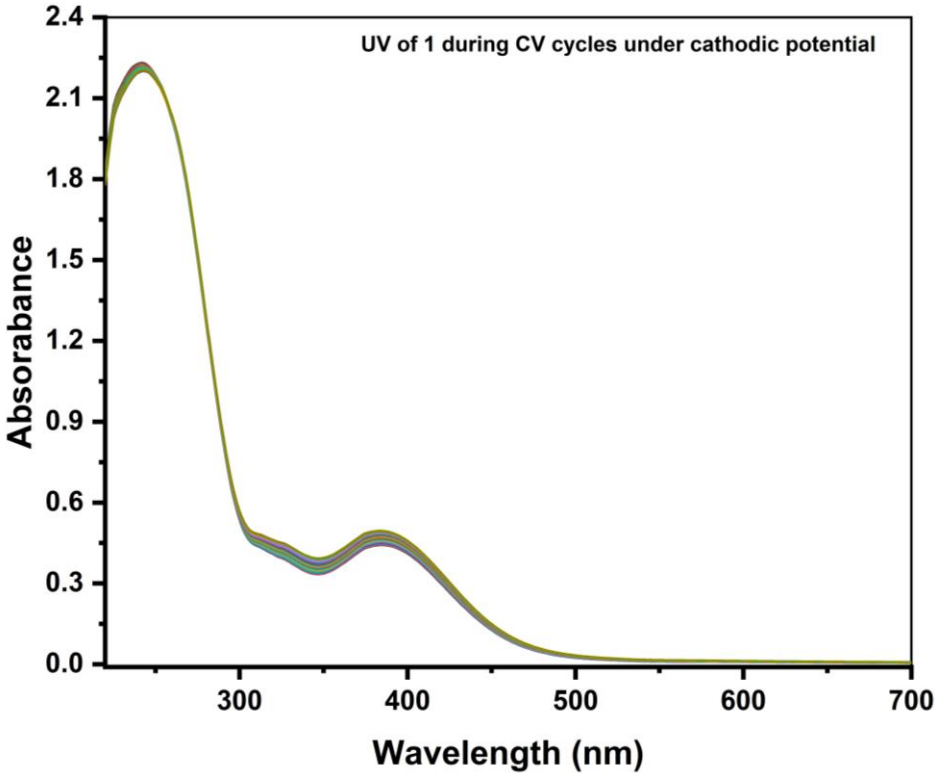

Figure S20. UV of **1** during continuous CV cycles under cathodic potential in the presence of 12mM acetic acid concentration using 0.1M $^{n}Bu_4NPF_6$ as a supporting electrolyte in methanol solvent.

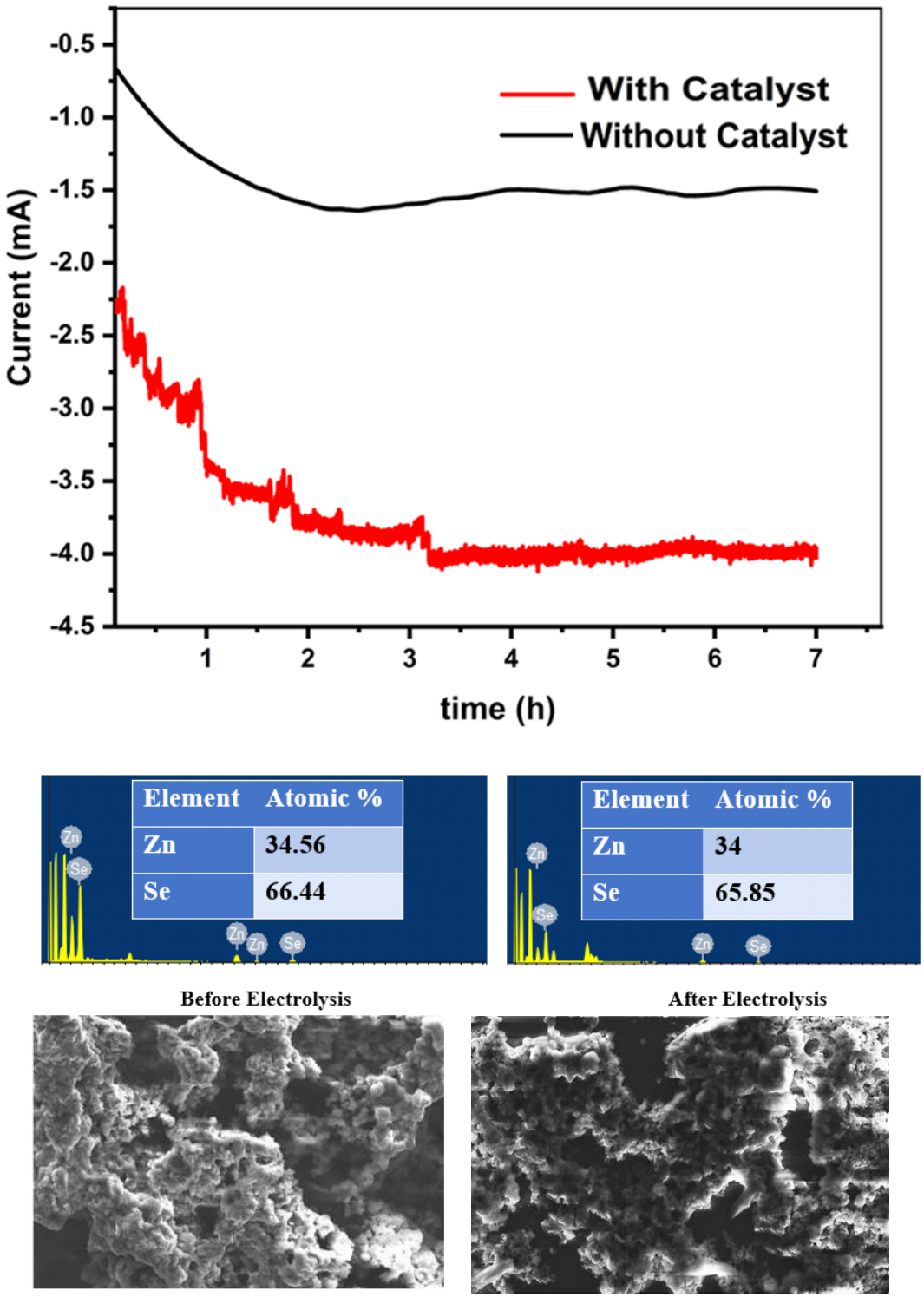

Figure S21. CPE study of the catalysis under heterogenous condition at GC electrode at -0.96 V *vs* Ag/AgCl (Upper). EDEX study and SEM image of the electrode surface before and after bulk electrolysis under anodic potential (Below).

Hydrogen-quantification and Faradic efficiency

In order to obtain experimental evidence that the evolved gas in the reduction of proton to hydrogen, we carried out the following dual reactions. The electrocatalysis reaction using the catalyst **1** was conducted in a gastight electrochemical cell through a cannula tube to another flask in which styrene and a catalytic amount of $RhCl(PPh_3)_3$ in benzene were placed. When the reaction was almost completed, ethylbenzene was produced in 15 % yield in the latter flask, demonstrating that the hydrogen gas generated in the former flask was transferred through the cannula tube to reduce styrene in the latter flask.

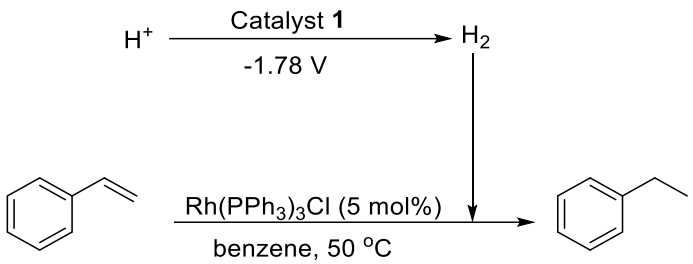

Scheme S2. Schematic representation of dual reaction.

Moles of ethylbenzene produced= 15 $x10^{-3}$ mmoles

Amount of hydrogen gas needed to reduced 1 mole of styrene = 1 mole H_2

Therefore, generated hydrogen during electrocatalysis = 15 µmoles

Total charge developed during electrolysis = 3.86 C

Faradic efficiency = 75 %

For Ligand: Moles of ethylbenzene produced= 4.41 $x10^{-3}$ mmoles

Amount of hydrogen gas needed to reduced 1 mole of styrene = 1 mole H_2

Therefore, generated hydrogen during electrocatalysis = 4.41 µmoles

Total charge developed during electrolysis = 2.96 C

Faradic efficiency = 28%

Hydrogenation of Styrene

Hydrogenation reaction was performed at constant pressure. In a typical run, the Wilkinson catalyst $Rh(PPh_3)_3Cl$ (0.005 mmol), styrene (0.1 mmol) and dodecane (0.03 mmol) were dissolved in benzene (1 mL) under a nitrogen atmosphere. The solution was then bubbled by hydrogen gas generated during water reduction. The temperature of the system was maintained at 50°C. After 12h, the reaction mixture was subjected to GC–MS analysis and showed quantitative conversion of styrene.

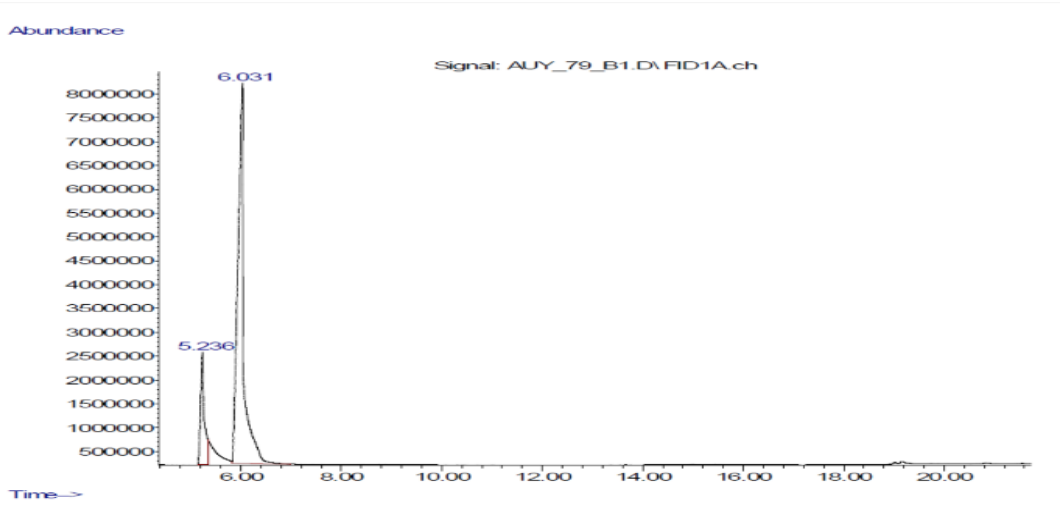

No peaks were detected using the method integration parameters!

Signal : AUY_79_B1.D\FID1A.ch

peak #	R.T. min	Start min	End min	PK TY	peak height	corr. area	corr. % max.	% of total
1	5.236	5.145	5.345	M	2350127	117230332	17.78%	15.093%
2	6.031	5.818	6.993	M	8228674	659497797	100.00%	84.907%

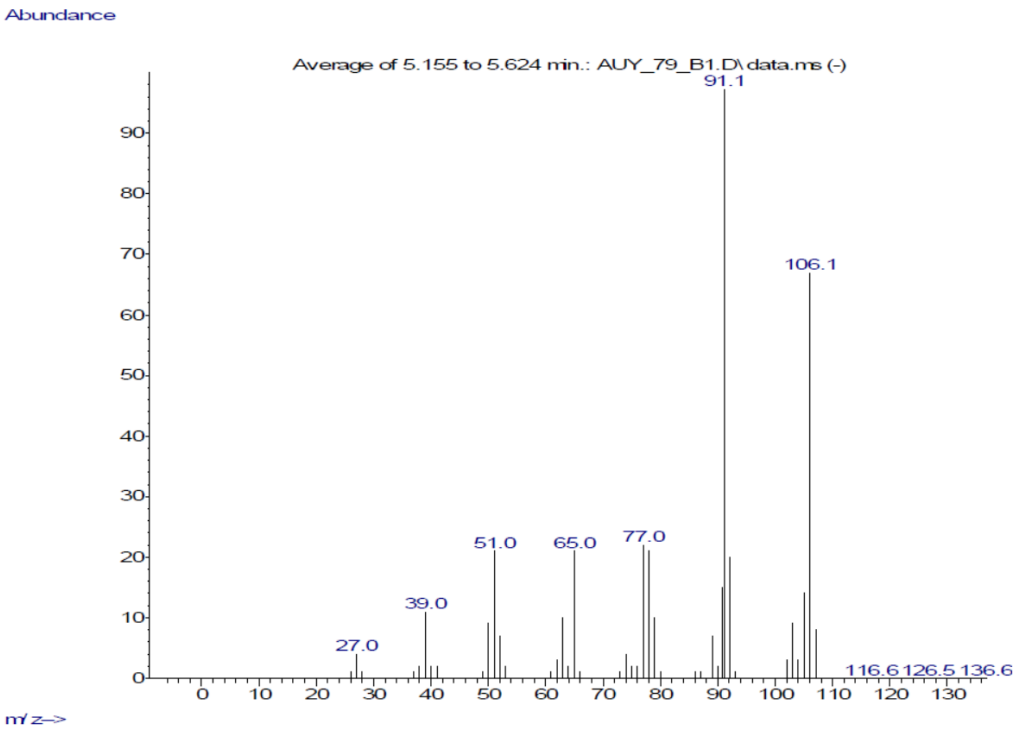

Figure S22. GC spectra of reaction mixture of styrene with hydrogen gas

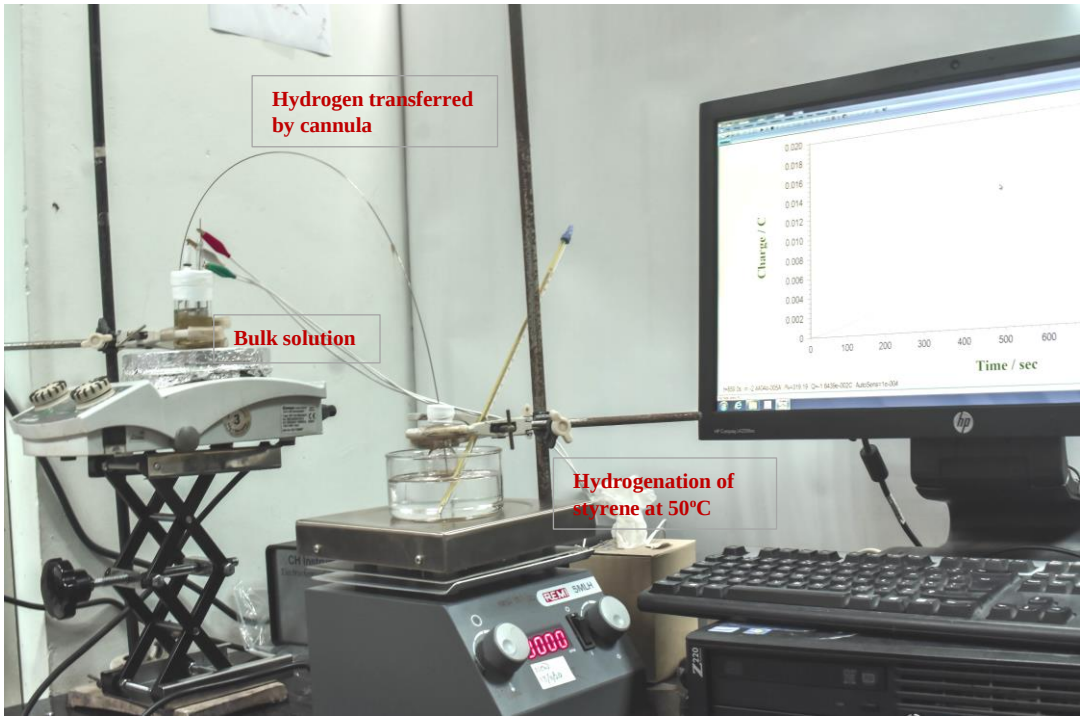

Figure S23. Reaction setup for the dual reaction.

Qualitative estimation of evolved hydrogen by GC thermal detector

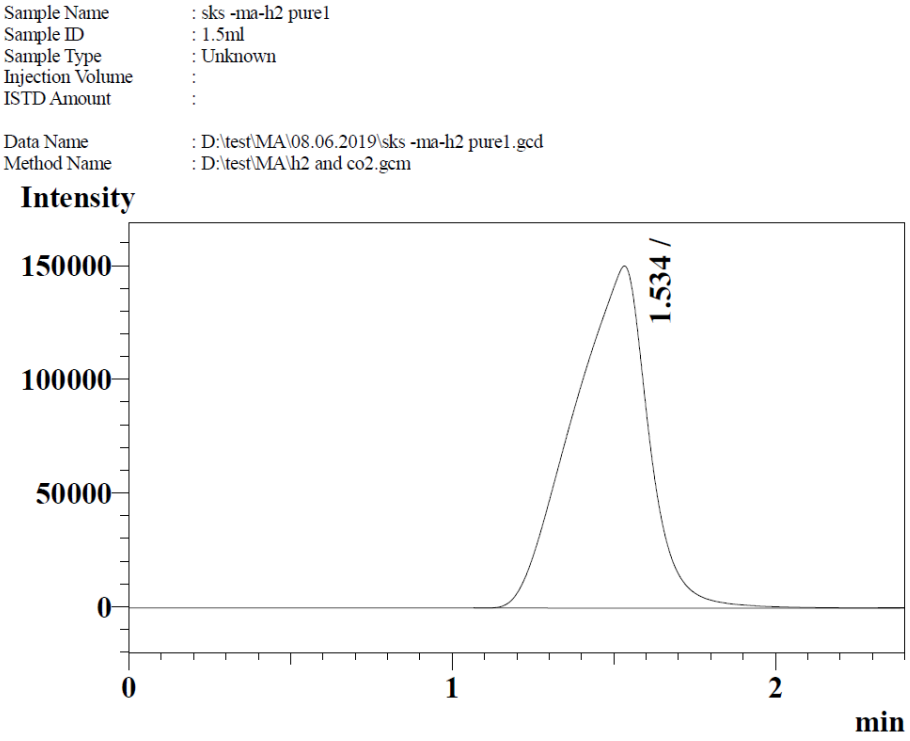

Figure S24. GC-TCD scan of pure hydrogen gas injected by Hamilton gas tight syringe.

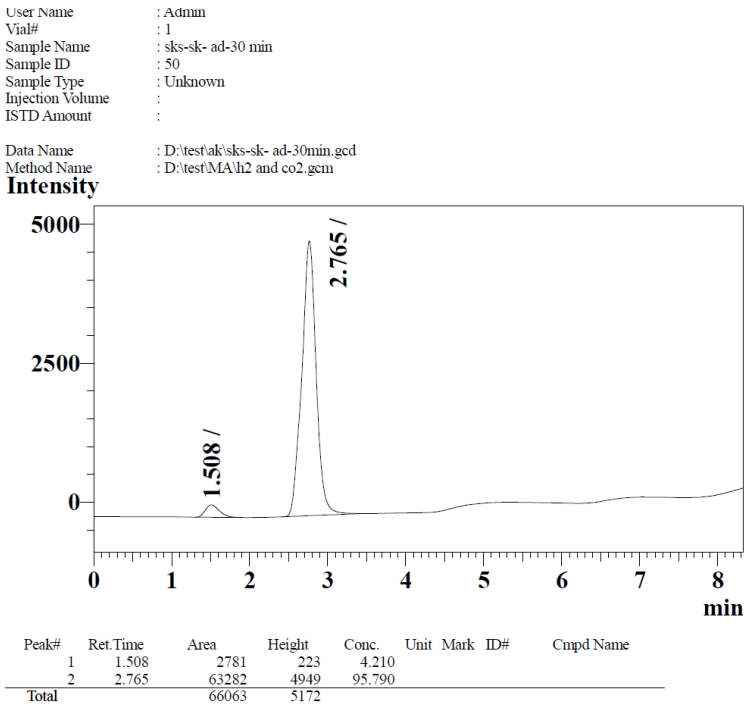

Peak#	Ret.Time	Area	Height	Conc.	Unit	Mark	ID#	Cmpd Name
1	1.508	2781	223	4.210				
2	2.765	63282	4949	95.790				
Total		66063	5172					

Figure S25. GC-TCD scan of evolved hydrogen gas after 30min bulk electrolysis of acid reduction. Reaction Condition: Catalyst **1** (3mM), acetic acid (12mM) in MeOH solvent using $^{n}Bu_4NPF_6$ (supporting electrolyte) at -1.78 V *vs* Ag/AgCl. electrolysis time= 30 minutes.

Post Electrolysis Dip Test

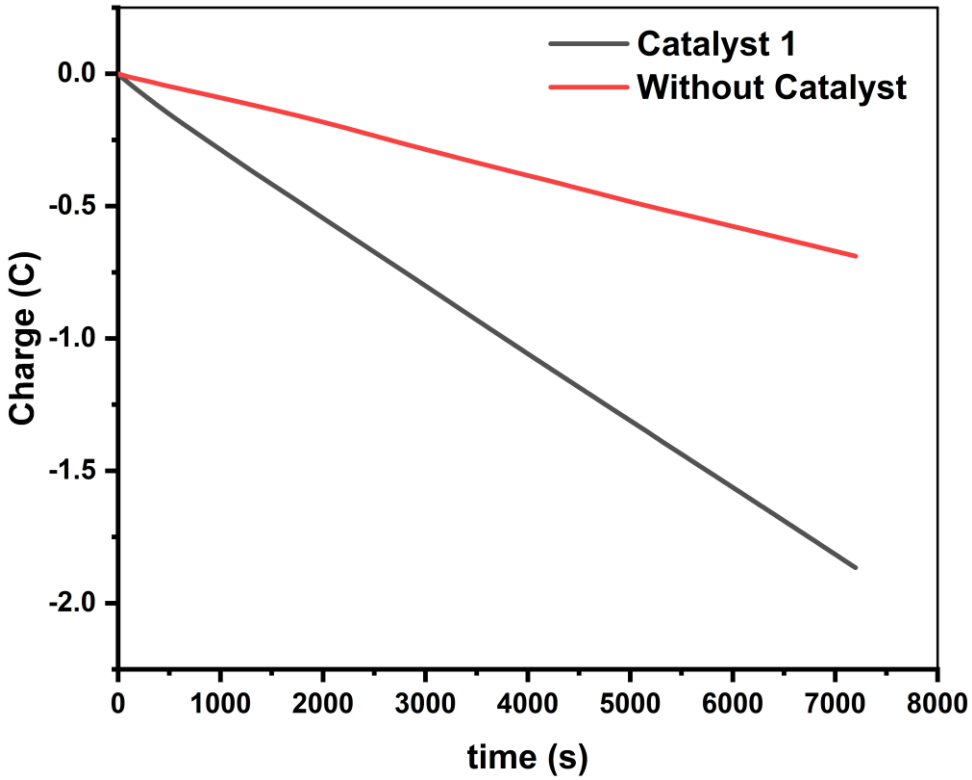

Figure S26. CPE for catalyst **1** (1mM), $^{n}Bu_4NPF_6$ (0.1M) in Methanol solvent with 12 mM acetic acid concentration at -1.85 V *vs* Ag/AgCl under cathodic potential. Black is with catalyst. Red is post run of black after rinse with deionized H_2O.

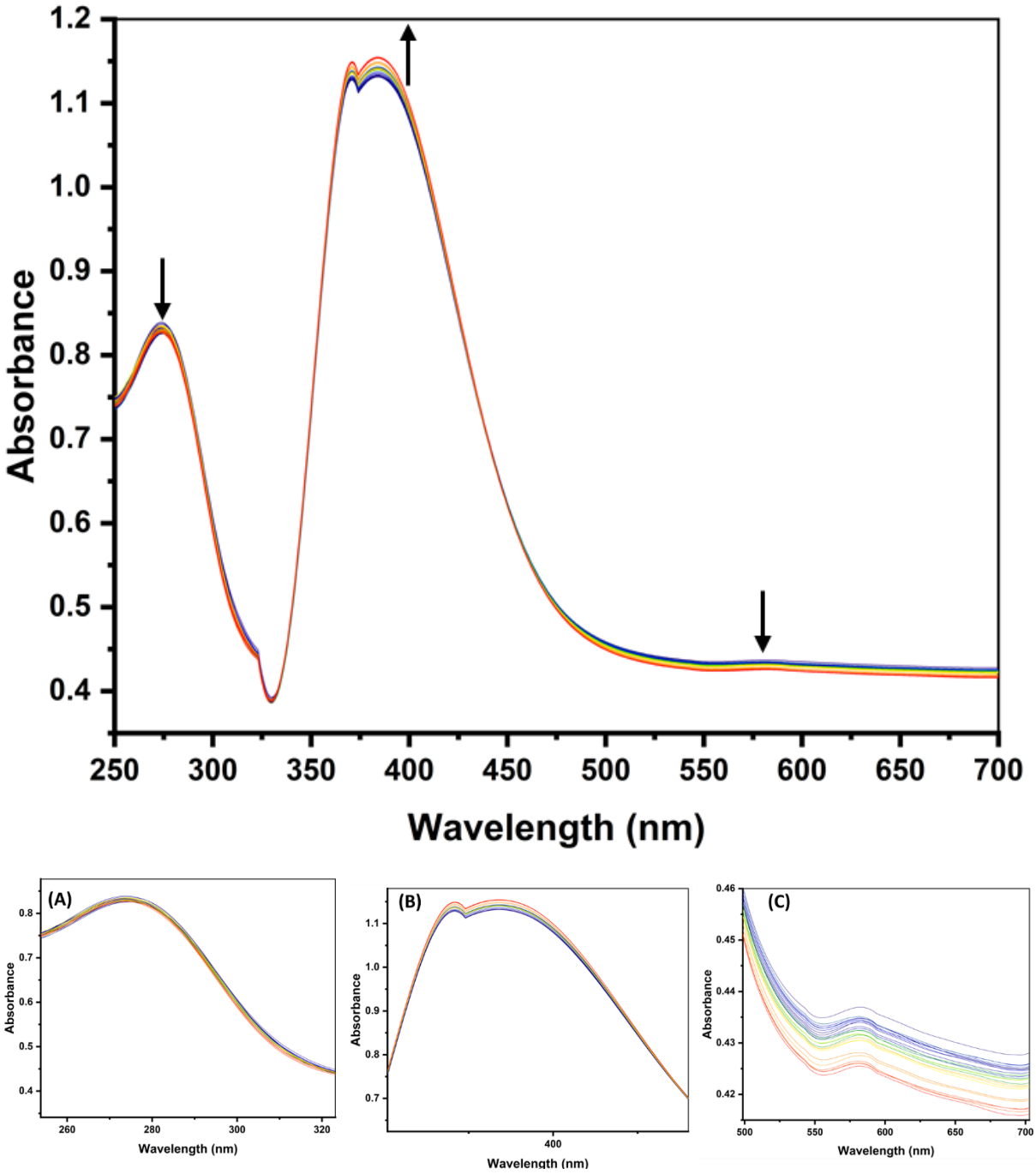

Figure S27. UV-visible spectra of zinc selenolate complex **1** from spectroelectrochemical electrolysis. UV spectra recorded during the electrolysis of 1 mM zinc selenolate catalyst **1** under applied potential of -1.85 V in 0.1 M $^{n}Bu_4NPF_6$ methanol solution. **Lowe**r: **(A)** and **(C)**, Decrease in absorption bands at 274 and 585 nm. **(B)** Blow up in the region of 342nm – 440nm region showing isosbestic point at 447 nm and 336 nm.

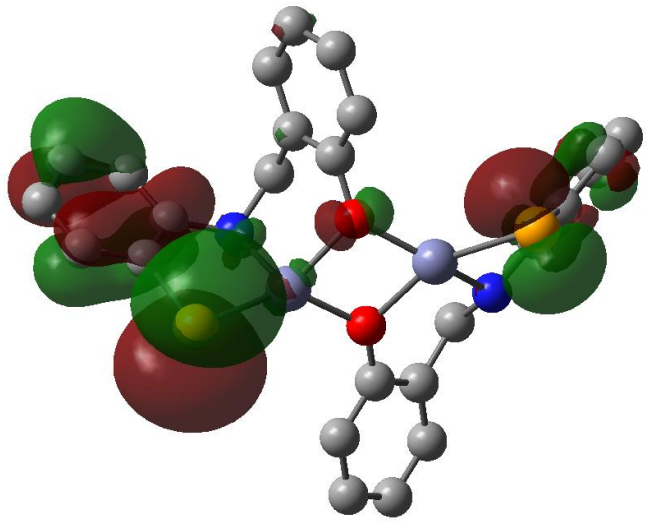

Figure S28. Highest occupied molecular orbital (HOMO) of bimetallic zinc selenolate **1**.

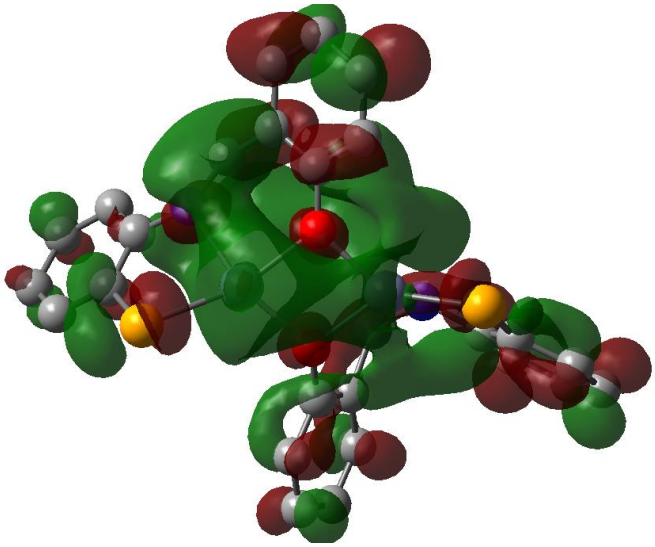

Figure S29. Lowest unoccupied molecular orbital (LUMO) of bimetallic zinc selenolate **1**.

Catalyst **1.2AcOH**: Calculated m/z = 803.8986

Experimentally observed: 803.2558

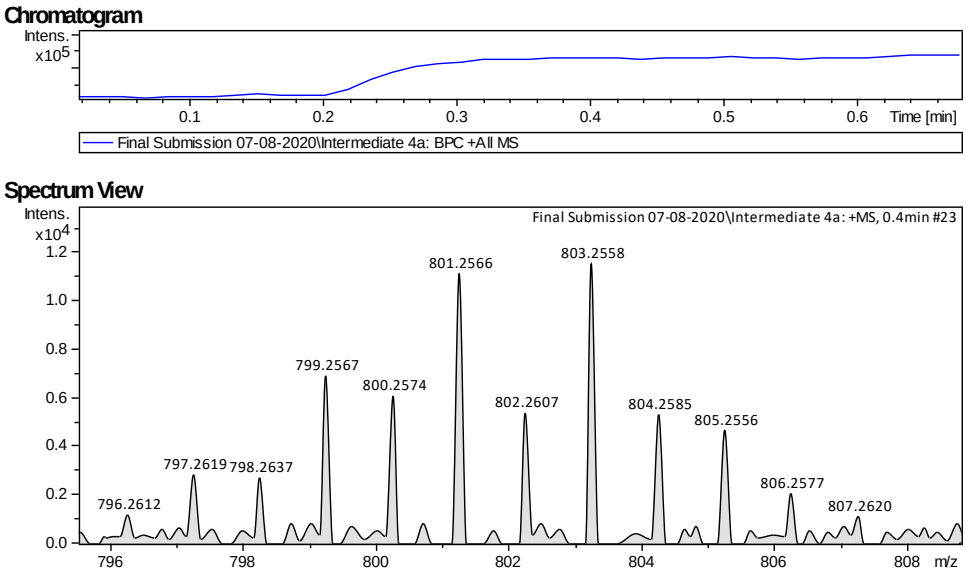

Figure S30. HRMS data of reaction mixture containing zinc selenolate 1 and acetic acid in methanol solvent.

DFT Calculations

All computational were performed with the Gaussian 09 Revision A.02 program suite[9] with the DFT method of Becke's three parameter hybrid Hartree-Fock procedure with the Lee-Yang- Parr correlation function (B3LYP). The geometry optimization calculation of the bimetallic zinc selenolate complex **1** was fully optimized by DFT/B3LYP method with the 6-311G(d) basis set in gass phase.

Table S1. Cartesian coordinates of optimized structure of 1.

Symbol	X	Y	Z
C	-5.74082	-1.31555	2.036952
C	-4.37681	-1.07298	2.145671
C	-3.6926	-0.35204	1.165943
C	-4.38624	0.153197	0.049429
C	-5.76335	-0.09591	-0.04202
C	-6.43373	-0.82168	0.933515
H	-6.25487	-1.88197	2.805994
H	-3.8395	-1.44745	3.010338
H	-6.30803	0.285276	-0.89869

H	-7.49881	-1.00309	0.8299
C	-1.38725	-1.18205	1.813778
H	-0.40663	-0.71474	1.950581
H	-1.71734	-1.52924	2.796238
C	-1.26265	-2.3473	0.866899
C	-0.62134	-2.16954	-0.37794
C	-1.69167	-3.62447	1.23299
C	-0.41069	-3.27288	-1.20996
C	-1.48854	-4.71968	0.398946
H	-2.18753	-3.76252	2.189926
C	-0.84026	-4.53729	-0.82169
H	0.094357	-3.11709	-2.15656
H	-1.82908	-5.70476	0.699141
H	-0.6712	-5.38425	-1.47928
N	-2.26348	-0.07263	1.311792
H	-2.16237	0.709302	1.956756
Se	-3.56817	1.200053	-1.36255
Zn	-1.47063	0.618822	-0.51702
O	-0.22404	-0.9301	-0.75211
O	0.283111	1.494849	-0.21577
C	0.607326	2.766418	0.110173
C	-0.16502	3.836671	-0.35886
C	1.724067	3.029628	0.93404
C	0.162507	5.147796	-0.03239
H	-1.03083	3.622114	-0.9772
C	2.040895	4.356991	1.236022
C	1.274225	5.417505	0.76259
H	-0.45135	5.960155	-0.40821
H	2.904076	4.560053	1.864371
H	1.53979	6.43865	1.013049
C	2.537447	1.907946	1.536204
H	1.932748	1.308588	2.225453
H	3.356965	2.34004	2.118979
N	3.051927	0.988908	0.496743
H	3.465866	1.543506	-0.25252
C	3.998641	-0.04183	0.865438
C	4.278811	-1.02282	-0.10986
C	4.601628	-0.10659	2.120753
C	5.205097	-2.02289	0.196395
C	5.508682	-1.12337	2.413565
H	4.375634	0.635344	2.877623
C	5.819006	-2.07307	1.444996
H	5.426096	-2.78007	-0.54764
H	5.971781	-1.1639	3.393743
H	6.527557	-2.86553	1.6634
Se	3.387102	-1.01097	-1.83045
Zn	1.535397	-0.00865	-0.71297

References

1. A. J. Bard, L. R. Faulkner, Electrochemical Methods: Fundamentals and Applications; Wiley: New York, 2001.
2. E. Laviron, *J. Electroanal. Chem.* 1979, **101**, 19 −28
3. J. M. Saveant, E. Vianello, *Electrochimica Acta* **1965**, *10*, 905–920.
4. A. D. Wilson, R. H. Newell, M. J. McNevin, J. T. Muckerman, M. R. DuBois, D. L. DuBois, *J. Am. Chem. Soc.* 2006, 128, 358–366.
5. A. M. Appel, D. L. DuBois, M. R. DuBois, *J. Am. Chem. Soc.* **2005**, *127*, 12717-12726.
6. Z. Chen, J. J. Concepcion, H. Luo, J. F. Hull, A. Paul, T. J. Meyer, *J. Am. Chem. Soc.* 2010, **132**, 17670–17673
7. S. J. Balkrishna, B. S. Bhakuni, S. Kumar, *Tetrahedron* 2011, **67**, 9565–.
8. V. Rathore, A. Upadhyay, S. Kumar, *Org. Lett.* 2018, **20**, 6274–6278.
9. M. J. Frisch, G. W. Trucks, H. B. Schlegel *et. al*. *Gaussian, Inc., Wallingford CT*, 2009